TECHNICAL PAPER

Different types of outrigger system in high-rise buildings: a preliminary comparative seismic analysis in a 40-story RC building

Aditya Kumar Tiwary[1,2]

Abstract

The rapidly growing number of high-rise structures around the world poses new obstacles, and lateral stiffness becomes one of the most critical issues as building height rises. The lateral stiffness and resistance capacity of high-rise buildings have a significant impact on structural efficiency, and structural engineers have introduced numerous capable constructions. The outrigger system is one of the most frequent and effective lateral loads resisting structural systems for improving structural stiffness and stabilizing the structure. The core shear wall provides structural strength in the main structural system, while the outrigger adds lateral stiffness. Several research on the outrigger system has been performed in previous studies, but a safe load transferring mechanism is the issue in the outrigger, as well as partial outrigger and belt depth, which has yet to be resolved. The concept of illumination and free space in outrigger structural systems is evaluated by comparing multiple outrigger system types utilizing a 40-story reinforced concrete building using ETABS 2017. The goal of this work is to do linear and dynamic (equivalent static and response spectrum) analyses, as well as nonlinear dynamic (time history) analyses of conventional outrigger, conventional outrigger with belt depth, virtual offset outrigger belt depth, conventional and virtual outrigger with partial depth under seismic load to better understand the performance and load transferring mechanism of distributed belt and conventional outrigger.

Keywords High-rise buildings · Outrigger · Time history analysis · Seismic

Introduction

The outrigger and belt truss system is a structural design that is commonly used to improve high-rise building lateral resistance to wind and seismic load [1–3]. As high-rise structures gain in popularity around the world, their impact on society and the economy has grown significantly. New high-rise construction frontiers will eventually complement rising needs for performance, efficacy, and cost-effective design. The rapid growth of the urban population as a result of economic activity and job opportunities places severe strain on limited land space, allowing for the construction of tall buildings [4]. A conventional outrigger is more robust

than a virtual outrigger since it has a straight load path, but it obstructs plane space and causes architectural disruption. Kashif et al. (2020) [5] investigated a high-rise building in both static and dynamic modes when subjected to lateral loads. The outrigger braced system was discovered to provide optimal control to high-rise structures under the same static loading. Arsalan et al. [6] suggested a stiffness-based technique for outrigger braced building preliminary design. Flexural rigidity of the core structure, outrigger belt height, and perimeter column diameters are all design variables. The comparative research demonstrated that the proposed technique gives a high level of accuracy in results [7–10].

Virtual, offset and braced outriggers, which are sufficient, eliminate the involute connection, and provide enough space, are introduced to solve these problems [11–13]. The approximation analysis of the RCC outrigger, which is employed in high-rise structures for design purposes under lateral distributed load, was discussed by Kafina and Sagaseta [14]. Han et al. [15] employed a gradient-based nonlinear programming approach to find the best locations for outriggers to reduce the top drift of tall buildings. By

✉ Aditya Kumar Tiwary
  adadtiwary15@gmail.com

1   Department of Civil Engineering, University Institute
    of Engineering, Chandigarh University, Mohali,
    Punjab 140413, India

2   University Centre for Research & Development, Chandigarh
    University, Mohali, Punjab 140413, India

modifying the cross-sectional area of outriggers, a series of optimum designs for three analytical models with varying vertical profiles were done to study the relationship between outrigger stiffness and optimum position. Outrigger stiffness in a practical range has no relationship with its optimal placement, and hence variables related to outrigger optimum location and stiffness can be examined separately for design purposes. For the core supported outrigger system and tube in a tube with an outrigger system, nonlinear finite element analysis is performed [15, 16]. The available approaches and formulas provide initial deflection and moment for core-outrigger and tube-in-tube outrigger systems but skip the reverse rotation of the outrigger [17]. Outrigger beam analysis shows that there are various load transformation paths that depend on reinforcement layout, with X-type reinforcement providing good overall performance [18]. Designers are worried about selecting structural solutions that can withstand lateral loads while still meeting serviceability and occupant comfort standards.

The impact of structural factors on the best position for the one-outrigger system in tall structures was investigated using MIDAS-Gen by Kim and Hyung-Kee [19]. The rigidity of major structural elements such as shear walls, outrigger systems, external columns connected in the outrigger system, and frames not to be connected in the outrigger system influenced the ideal location of the one-outrigger system, according to the conclusions of this study. Furthermore, the findings of the study have been shown to be particularly valuable in acquiring structure design data for determining the optimal position for a one-outrigger system in a high-rise building [19]. In high-rise structures, increasing the number of outriggers reduces the maximum differential axial shortening, but when the number of outriggers is raised by more than two, there is no significant reduction in differential axial shortening. According to the data, outrigger has been recognized as an extraordinarily effective arbiter in a mutual dialogue. The complexity of tall structure design continues to be a difficulty due to earthquakes and wind [20, 21].

The distributed belt wall system, developed by Eom et al. [22], is a novel lateral force-resisting structural technique for concrete high-rise buildings. Unlike conventional belt systems, the belt walls that fill the gap between perimeter columns are distributed independently across the height of the building. The dispersed belt wall system, which consists of belt walls that are not directly coupled to the core wall and act as virtual outriggers, has been found to be just as effective as traditional belt and outrigger systems in preventing lateral drift of high-rise buildings. The number and arrangement of belt walls affect the performance of a distributed belt wall system [22–25].

To eliminate differential axial shortening, Kim [26] investigated the optimal outrigger position in reinforced concrete

high-rise buildings and worked on an 80-story reinforced concrete structure built to withstand lateral loads, wind, and earthquake forces. To simulate the three models with various sectional profiles, the authors used a reinforced concrete core with a single multi-story outrigger at every point throughout the height of the structure, and it was observed that differential axial shortening and its effects should be considered in the design. The ideal location for the outrigger is one that reduces the peak of excessive differential axial shortening. The analytical study of the most effective conventional outrigger and virtual outrigger system to resist lateral load was conducted in the previous study [27, 28].

The research gap exists regarding the depth of the distributed belt wall when acting as a virtual outrigger, a conventional outrigger, and a partial depth increment of both conventional and virtual outriggers. The load-transferring system for the RCC building's distribution belt wall and outrigger is not described in enough detail. Additionally, a limited investigation was performed on a specific type of outrigger system that makes up for the lack of illumination and free space. This study aims to find the safest load-transmitting path for the outrigger system in reinforced concrete structures as well as the most effective outrigger system with regard to depth. Additionally, the ideal outrigger system, which offers adequate free space and lighting at the outrigger level, was obtained. To better comprehend the performance and load-transferring mechanism of distributed belts and conventional outriggers under seismic load, linear static and dynamic analyses (equivalent static and response spectrum), as well as nonlinear dynamic (time history) analyses, were conducted. Based on the research of numerous types of outrigger systems using ETABS 2017 [29] on a 40-story reinforced concrete building, the perception of illumination and free space in outrigger structural systems was determined.

Effect of the core outrigger and exterior columns interaction at different heights

Three-quarter height from bottom

Figure 1 depicts the interactions between the core, outriggers, and external columns, which are described in detail using analytical methodologies and a common equation for lateral deflection of a cantilever exposed to lateral stress [30].
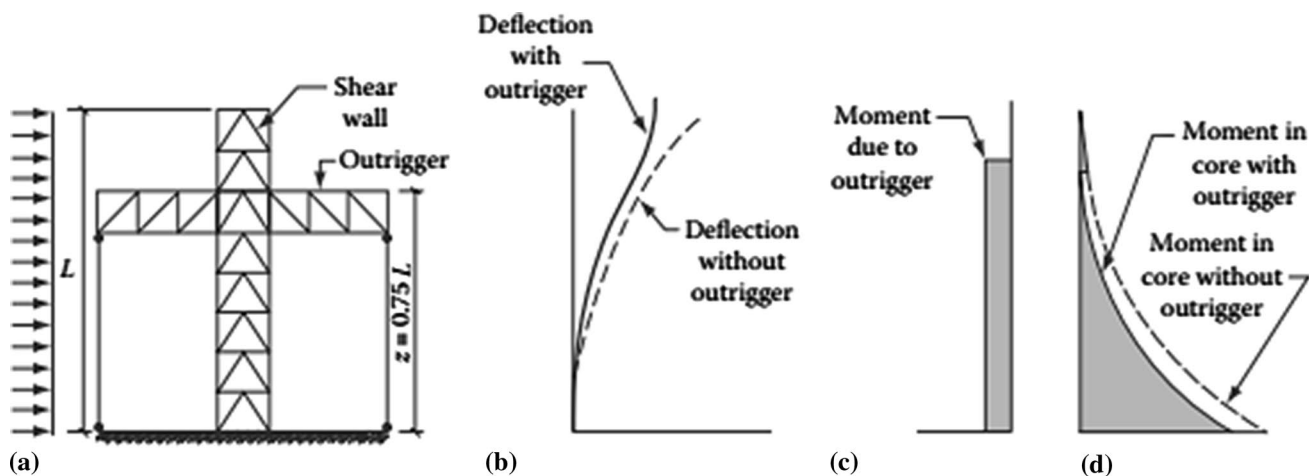
$$y = \frac{W}{24EI}\left(x^4 - 4xL^3 + 3L^4\right) \tag{1}$$

Fig. 1 **a** Analytical model **b** deflection **c**, **d** moment diagrams (Taranath, 2016)

where x is the distance from the top, L is the length, w is the load, and EI is the flexural rigidity.

The general equation of slope for cantilever by differentiating respect to x

$$\frac{dy}{dx} = \frac{W}{6EI}\left(x^3 - L^3\right) \tag{2}$$

The outrigger slope location is certain by substituting $Z = 3L/4$ and $x = L/4$.

$$\frac{dy}{dx}\left(\text{at } z - \frac{3L}{4}\right) - \frac{W}{6EI}\left(\frac{L^3}{64} - L^3\right) = \frac{WL^3}{6EI} \times \frac{63}{64} \tag{3}$$

By representation M_2 and K_2 as moment stiffness of outrigger at $Z = 3L/4$, so the compatibility equation at Z can be expressed as:

$$\frac{WL^3}{6EI}\left(\frac{63}{64}\right) - \frac{M_2}{EI}\left(\frac{3L}{4}\right) = \frac{M_2}{K_2} \tag{4}$$

By adding $K_2 = 4K_1/3$, the M_2 can be written as:

$$M_2 = \left(\frac{WL^3/6EI}{1/K_1 + L/EI}\right)1.31 \tag{5}$$

$$M_3 = 1.75M_1 \tag{6}$$

The drift can be written as:

$$\Delta_2 = \frac{WL^4}{8EI} - \frac{M_3 L}{2EI}\left(L - \frac{L}{4}\right) = \frac{L^2}{2EI}\left(\frac{WL^2}{4} - 1.23M_1\right) \tag{7}$$
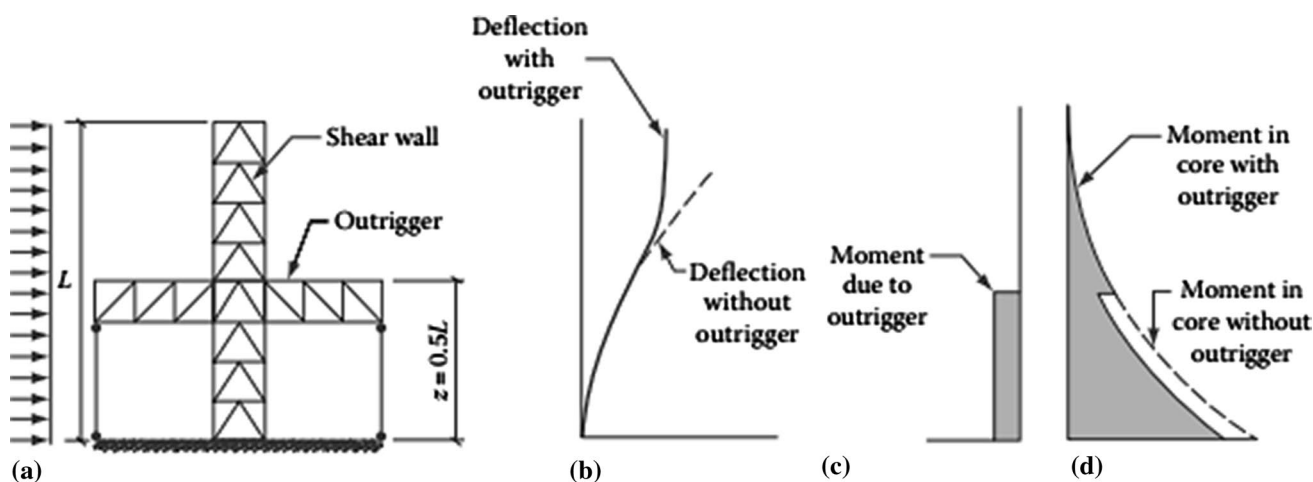
Fig. 2 **a** Analytical model **b** deflection **c**, **d** moment diagrams (Taranath, 2016)

Mid height

Core outrigger and exterior columns interaction effect at mid-height is shown in Fig. 2. Due to exterior load $W = 7WL^3/48EI$ and rotation at $Z = L/2$, the rotation compatibility expression is expressed as [30]:

$$\frac{7WL^3}{48EI} - \frac{M_3L}{2EI} = \frac{M_3}{K_3} \tag{8}$$

By representation of M2 and K2 as moment stiffness of outrigger at $Z = L/2$ and the $K_3 = 2K_1$, M3 can be expressed as:

$$M_3 = \left(\frac{WL^3/6EI}{1/K_1 + L/EI}\right) \times \frac{7}{4} = 1.75M_1 \tag{9}$$

Drift is equal to:

$$\Delta_3 = \frac{WL^4}{8EI} - \frac{M_3L}{2EI}\left(L - \frac{L}{4}\right) = \frac{L^2}{2EI}\left(\frac{WL^2}{4} - 1.31M_1\right) \tag{10}$$

Recommendation of optimum location for outrigger system

The primary goal of using outriggers is to offer occupants with comfort and a sturdy structure by limiting lateral deflection, story drift, and overturning moments. There has been numerous research on outrigger location and number in high-rise structures, all of which show that outriggers play an important role in the structural performance of tall structures:

- When a single outrigger is located at the top of the structure, lateral drift is reduced by 50%, whereas when an outrigger is located at mid-height, lateral drift is reduced by 75%. Architectural preferences, on the other hand, take precedence in terms of building layout, with the single outrigger preferred location at the top.
- The use of two outriggers provides a variety of possibilities for outrigger positioning, which provides structural stability in the form of deflection, as shown in Fig. 3. Two outriggers should be positioned at h/3 and 2 h/3 of the height, three outriggers at h/4, h/2, and 3 h/4 of the

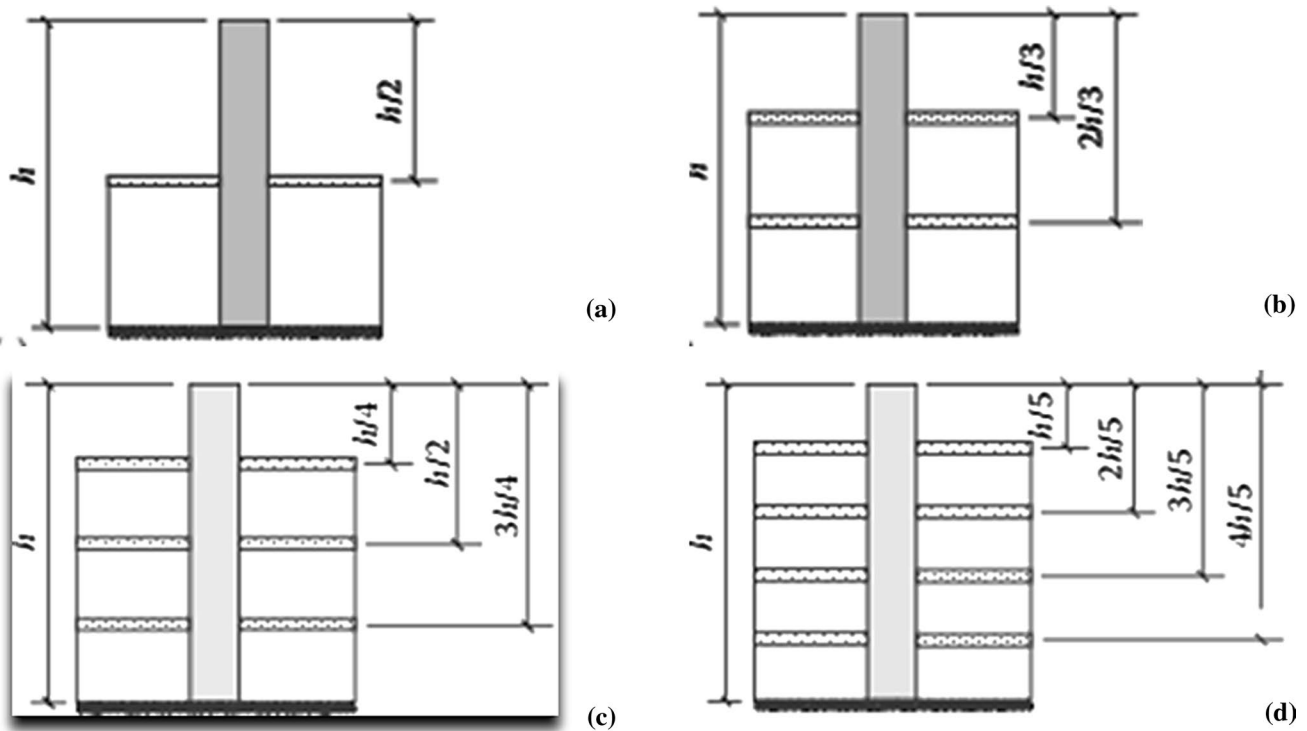**Fig. 3** Optimum location for **a** single outrigger, **b** double outriggers, **c** three outriggers, **d** four outriggers

height, and four outriggers at h/5, 2 h/5, 3 h/5, and 4 h/5 of the height [30].

Types of analyses

Various forms of lateral load resisting systems, such as moment frame, bracing system, shear wall system, core system, core-outrigger system, tube, tube in tube, bundle tube, and diagrid system, have been covered for all typical and exceptional structural systems for high-rise structures. In this paper, the moment frame, bracing system, shear wall, core, and outrigger were employed in conjunction. Outrigger combined with mentions system has been studied with a different configuration, and all load combinations and required data must interoperate based on analysis results. Models of 40 stories with a total height of 120 m have been used, although with a different outrigger design. A 36×36 m square-shaped plan was used to compare the efficiency of various types and configurations of outrigger systems. The structural analysis software ETABS 2017 [29] was used to assess all models utilizing static and dynamic methods under seismic load.

Equivalent static method

It's a sort of linear static analysis that's also known as the coefficient static method, and it's used to calculate lateral design forces. It is a widely used method for both irregular and regular structures that requires less effort; the corresponding static method is based on code-presented formulas. To begin, all models will be analyzed using an equivalent static method, which calculates the weight and lumped of the structure and distributes it evenly on the floors. Next, base shear will be calculated using a code-based formula, and this base shear will be distributed to all members based on their relative stiffness. According to IS1893 (part 1):2016 [32] clause 7.5.2, the design seismic base shear is as follows:

$$V_B = A_h \times W \tag{11}$$

A_h = design horizontal acceleration spectrum value as per 6.4.2 (IS 1893):2016, T_a as per clause 7.6 fundamental natural period, W = seismic weight of structure, design base shear shall be distributed as per below equation

$$Qi = V_B \left(\left(Wi \times Hi^2 \right) / \left(\sum_{j=1}^{n} \left(Wj \times Hj^2 \right) \right) \right) \tag{12}$$

Qi = Design lateral force at i floor, Wi = seismic weight of i floor, Hi = height of floor, n = number of stories in structure.

Response spectrum analysis

It is a plot of the maximum response of a linear single degree of freedom oscillator for a specific component of seismic ground motion; the natural period is on the x-axis, and the response amount is on the y-axis. Aside from a certain restriction, increasing the height of the building is insufficient, and a dynamic study is required. All structures in the IV and V zones shall be dynamically assessed, according to paragraph 7.8.1 of IS 1893 (part 1):2016 [32]. Because the models utilized in this study all have a height of about 120 m, they should be dynamically examined. The extreme response of a structure is obtained directly from the seismic response spectrum in this method, and structure-response is viewed as manifold modes for seismic. Using model combination methods, each mode response was merged to obtain the structural response (Square Root of Sum of Squares and Complete Quadratic Combination). In this research, we look at the CQC approach for combining modes [21].

Time history analysis

It is a nonlinear dynamic analysis, which is the dynamic response of a structure for each increment of time when its base is exposed to a known ground motion time history. Time history is a multi-degree of freedom system application. Those models that perform better in equivalent static and response spectrum analysis will be analyzed using seismic (El Centro) time history analysis to determine which structural system is the best [21].

Analyzed buildings

The current analysis considers a multi-story symmetrical office reinforced concrete (RC) structure in Chandigarh, which is presumed to be in zone IV. According to the study's objectives, all models will be analyzed using the response spectrum method to assess the performance and proficiency of various types of outrigger systems, and the best structures among them will be analyzed for time history to assess the structure's behavior in severe and real seismic events. All 34 models that have been modeled with ETABS 2017 [29] are divided into six categories for simple comprehension.

Property

The dimensions of the structural system were 36 m×36 m, with the number of bays and bay spans in both horizontal

directions kept constant to persuade. The study includes 34 models, with all of the analytical models having 40 stories and a constant story height of 3 m. Analytical models do not represent any type of structure in the real world. However, the quality, size, and overall layout have been chosen to be representative of an outrigger building in accordance with Indian standards. All models were made the same size and with the same material attributes throughout the height.

In all versions, M40 grade of concrete and Fe-415 steel were utilized, with concentric (X) type bracing. The concrete grade for the structure was chosen in accordance with the code; according to clause 5.2 of IS 13920–2016 [31], the minimum concrete grade for buildings located in seismic zones III, IV, and V and having a height of more than 15 m should be M20, but M25 for buildings located in seismic zones III, IV, and V and having a height of more than 15 m should be M25. However, for the current investigation, grade M30 concrete has chosen to design using the trail and pass all fail members. According to the code, steel reinforcement for structures shall employ grade Fe-415 or less, with grades Fe-500 and Fe-550 as a second choice, as per clause 5.3.1 of IS 13920–2016 [31]. Steel reinforcement of minimum grade Fe-415 was employed in the current investigation. Beams dimensions have also designated according to code, as per clause 6.1.1 IS 13920–2016 [31] beam must favorably have width/depth > 0.3 or beam width shouldn't smaller than 200 mm or beam depth shouldn't be more than $D < 1/4th \times$ clear span. As per clause 3.2.1, IS 13920–2016 [31] deflection control for beam recommends that span/depth > values and these values are 7, 20 and 26 for cantilever, simple supported and continues beams, respectively. Beams, which have used for this study, fulfill all the requirement of code. Columns dimensions have also designated according to code, as per clause 7.1.1 IS 13920–2016 [31], minimum dimension of the column shouldn't be smaller than $\geq 20 \times$ dia of longitudinal bar or ≥ 300 mm, and according to clause 7.1.2 IS 13920–2016 [31] the cross-sectional aspect ratio shall not be less than $a/b > 0.45$ and column has provided according to rule for the current study. The performance of bracing is dependent on the cross-section size and configuration, but bracing improves the structure's capability in terms of strength, deformation, and ductility when compared to no-bracing, and the X bracing system outperformed others by increasing drift control and ductility by increasing dimensions, resulting in better performance. The geometric properties of buildings are listed in Table 1.

According to 1893(part1):2016 [32], every conventional construction with a height of greater than 40 m in zones IV and V requires a dynamic study because all models have a

constant height of 120 m. ETABS v17 [29] was used to analyze the models, which included linear static and dynamic (equivalent static and response spectrum) techniques as well as nonlinear dynamic (time history) techniques. The models were compared in terms of lateral displacement, maximum time period, story drift, and base shear parameter. Because the construction is expected to be in Chandigarh's seismic zone IV, the seismic parameters were specified in accordance with the regulations. Clause 6.4.2 of the IS 1893–2016 [32] standard specifies the zone factor, importance factor, and response reduction factor considered as listed in Table 2.

According to IS 875 (part 1)-1987 [33], the dead load was taken as listed in Table 3. The live load was chosen based on the IS 875 (part 2)-1987 [34] code for an office building.

For all models throughout the height of the structure, two outriggers were employed: one at H/3 and the other at 2H/3 [30]. The response spectrum has increased to almost 85% of total static base shear.

Outriggers modeling

Conventional outrigger

In this scenario, seven structural models with various outrigger configurations, concrete, and steel specifications with

Table 1 Geometric parameters

Sr.no	Beam (mm)	Column (mm)	Thickness of shear wall (mm)	Slab thickness (mm)	Bracing type
1	500×350	800×800	300	150	ISHB 450–2

Table 2 Seismic parameters

Sr.no	Importance factor (I)	Zone factor (Z)	Response reduction factor(R)	Type of soil	Damping ratio
1	1.5	0.24	5	II	5%

Table 3 Loadings

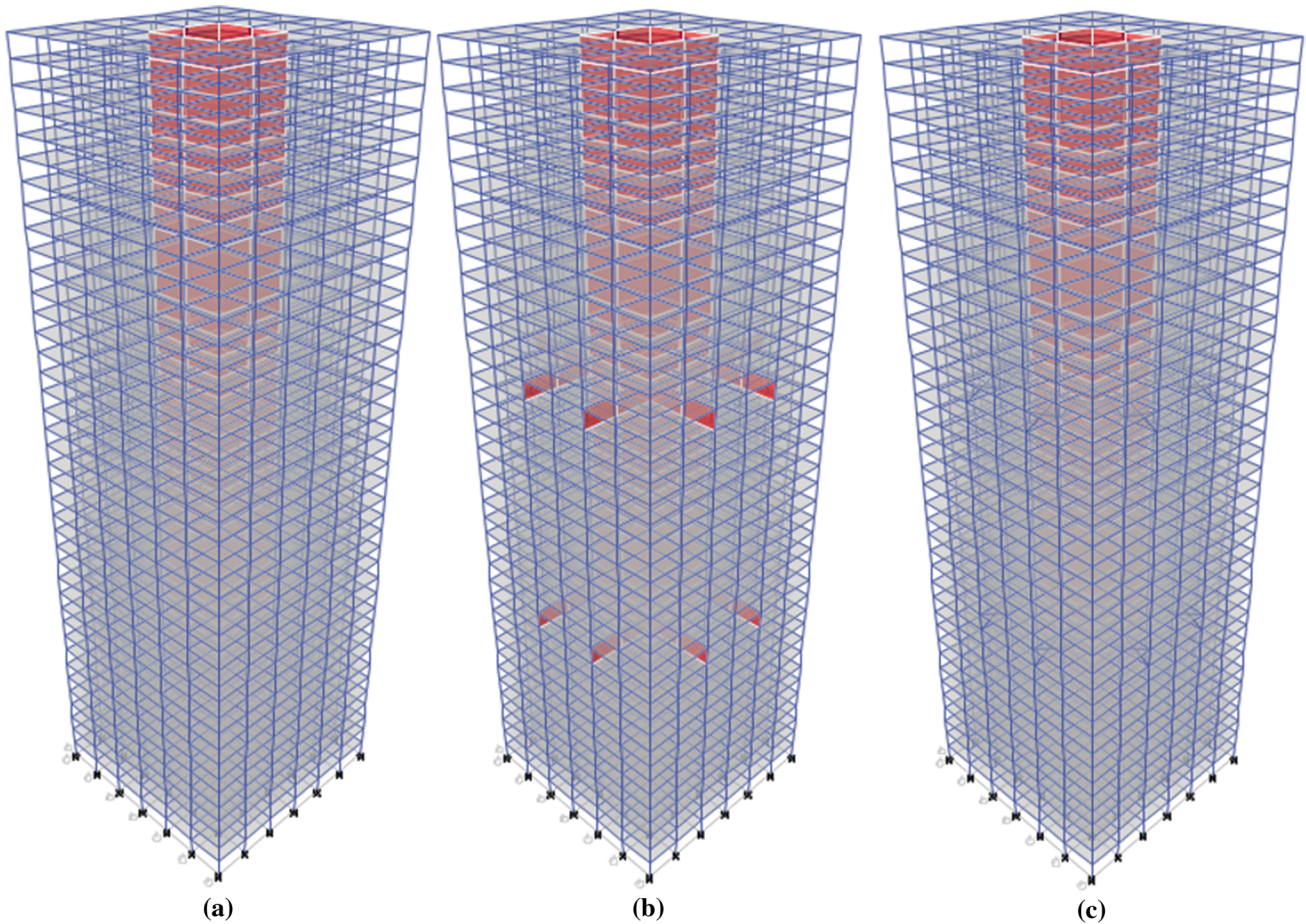| Sr.no	Live load (kN/m²)	Super dead load (kN/m²)
1	3	1

Fig. 4 Building frame with **a** core, B2, **b** wall outrigger, B3, **c** braced outrigger, B4

variable positions for the outrigger and belt trusses were examined. As shown in Figs. 4 and 5, the (B2) model has only a shear wall core, (B3) model has only a shear wall outrigger, (B4) model has only an X-braced outrigger, (B5) model has a shear wall outrigger and belt wall, (B6) model has shear wall outrigger and X-braced belt, (B7) model has X-braced outrigger and wall belt. The outrigger wall's height is equal to the floor height (3 m), and the belt wall's height is the same for all models. Other geometric properties, loads, seismic characteristics, plan, and height are all the same.

Conventional outrigger with belt depth

In this case, twelve structural models were examined with varying outrigger belt depths. Concrete and steel were

employed for the belt. The height of the outrigger wall is the same as the floor height (3 m), while the height of the belt wall ranges from a single story (3 m) to a triple story (9 m), and all other geometric properties, loads, seismic characteristics, plan, and height are consistent throughout all models. Figures 6, 7, and 8 show (B8) the model with shear wall outrigger and single-story belt wall, (B9) the model with shear wall outrigger and double-story belt wall, (B10) the model with shear wall outrigger and triple-story belt wall, (B11) the model with shear wall outrigger and single-story X-braced belt, (B12) the model with shear wall outrigger and double-story X-braced belt, (B13) the model with shear wall outrigger and triple-story X-braced belt, the model with an X-braced outrigger and double-story X-braced belt (B14), and the model with an X-braced outrigger and triple-story X-braced belt (B15).
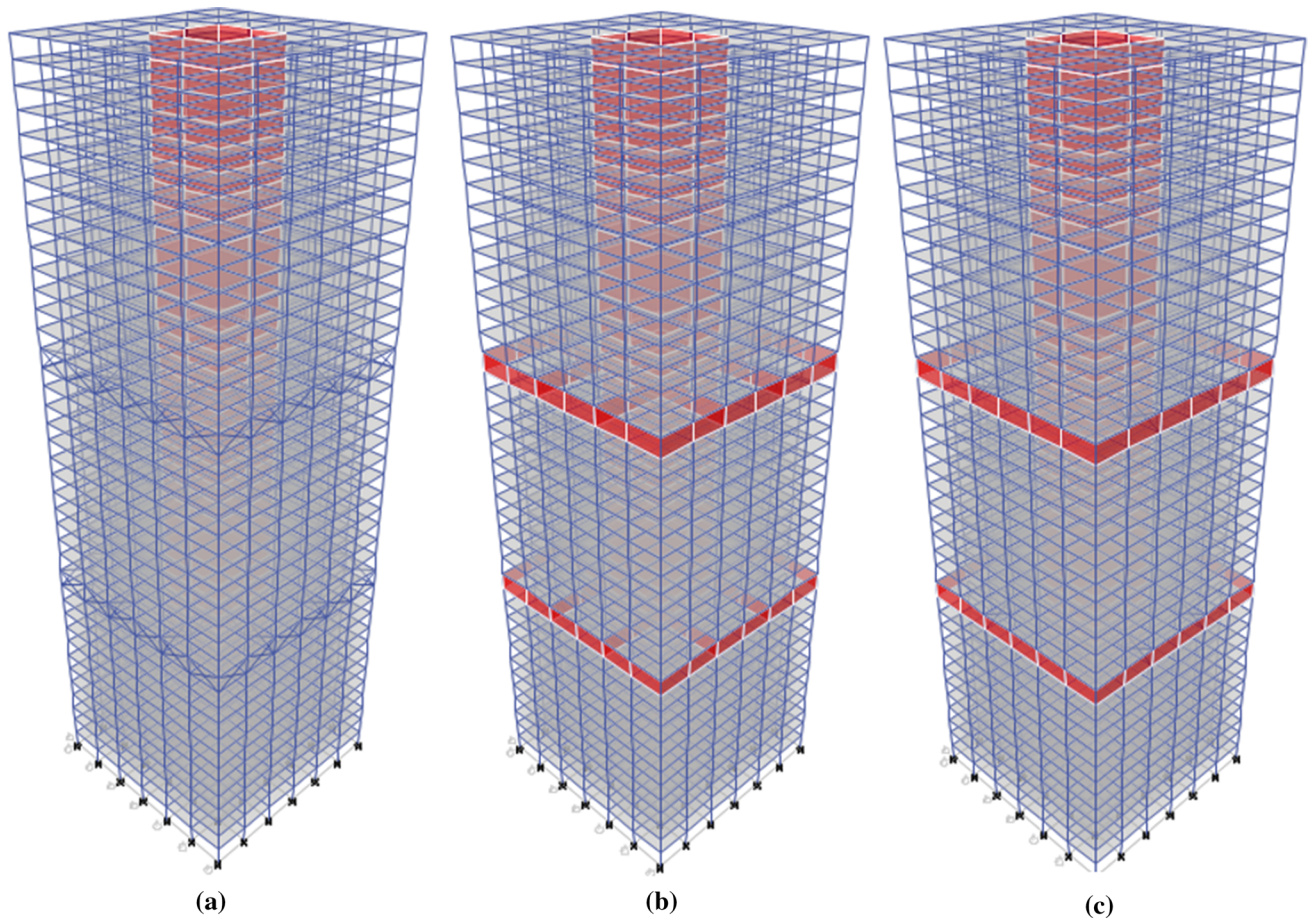
Fig. 5 Conventional frame with **a** braced outrigger with brace belt, B5, **b** wall outrigger with wall braced, B6, **c** braced outrigger with wall belt, B7

Virtual offset outrigger with belt depth

In this scenario, twelve structural models with various outrigger configurations, concrete, and steel with variable positions for the belt trusses were examined. An offset virtual outrigger is a new form of outrigger that considers the use of concrete and steel. Outrigger wall height is identical to floor height (3 m), and belt wall height varies from single-story (3 m) to triple-story (9 m), but offset outrigger has a single-story belt (3 m), and all other geometric properties, loads, seismic characteristics, plan, and height are the same for all models. Figures 9, 10, 11, 12, 13, and 14 show the models (B16) single-story belt wall, (B17) double-story belt wall, (B18) triple-story

belt wall, (B19) single-story X-braced belt, (B20) double-story X-braced belt, (B21) triple-story X-braced belt, (B22) single-story inner wall outrigger, (B23) with single-story outer wall outrigger, (B24) with single-story inner X-braced outrigger, (B25) with single-story outer X-braced outrigger, (B26) with single-story double-wall outrigger, and (B27) with single-story double X-braced outrigger.

Virtual outrigger with partial belt depth

In this case, six structural models with various outrigger configurations, concrete, and steel with partial depth in the outrigger and belt were investigated. The height of
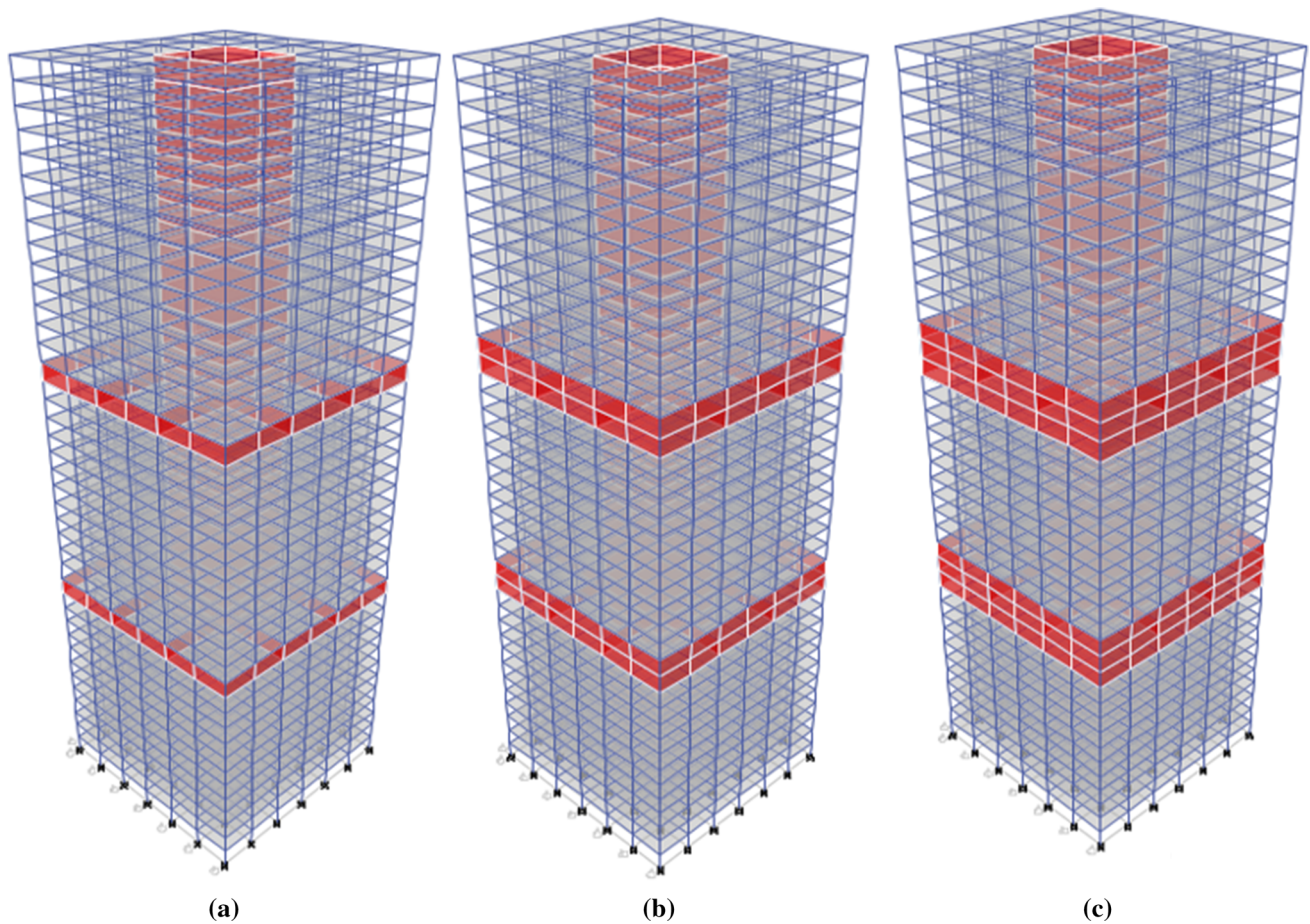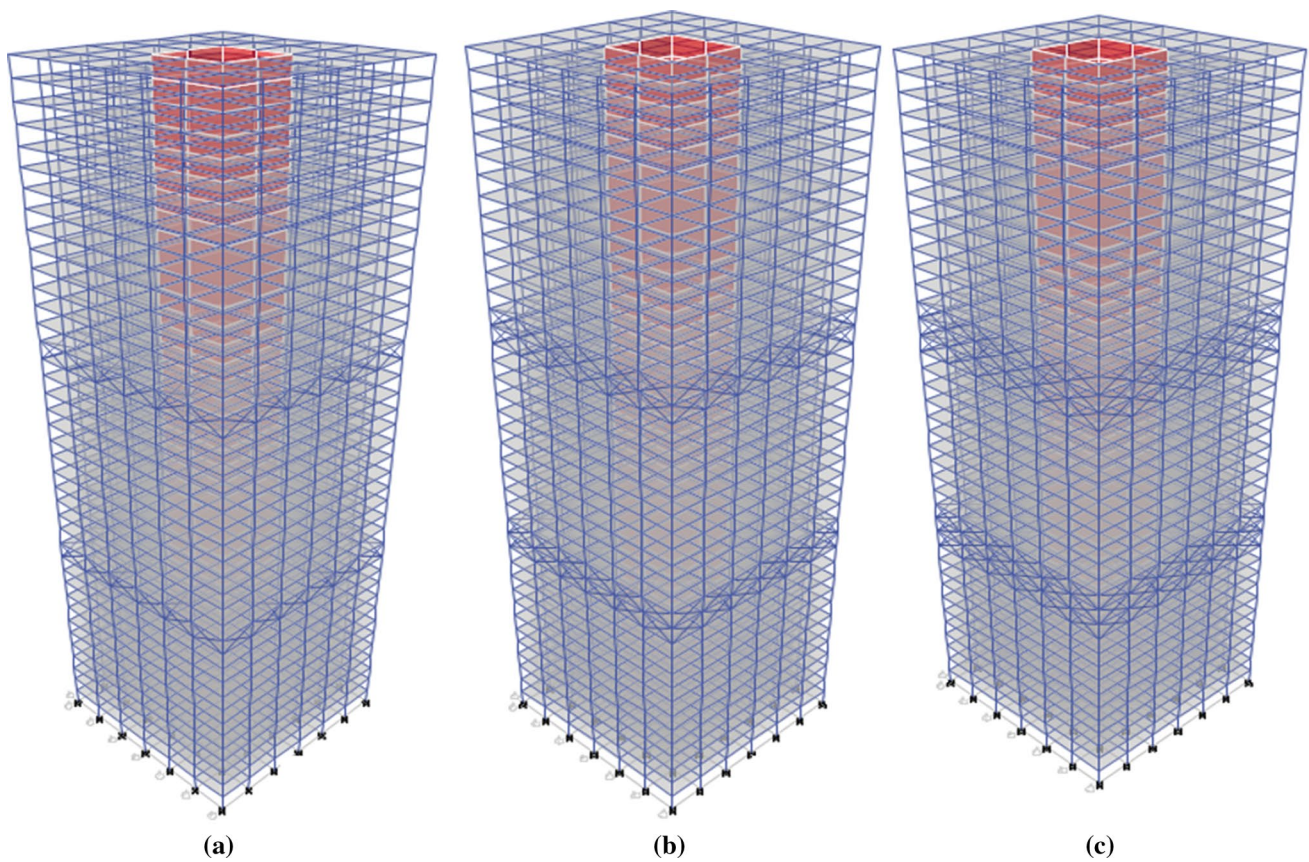
Fig. 6 Conventional wall outrigger with **a** single-story wall belt depth, B8, **b** double-story wall belt depth, B9, **c** triple-story wall belt depth, B10

the outrigger wall is the same as the floor height (3 m), but the partial depth rises to 9 m, and the height of the belt wall has a single-story belt (3 m), but the partial depth rises to 9 m. Another geometric property, however, is that all models have the same loading, seismic parameters, plan, and height. Figures 15, 16, 17, 18, 19, and 20 illustrate (B28) model of partial increment wall outrigger, (B29) model of partial increment X-braced outrigger, (B30) model of partial increment wall outrigger and wall belt, (B31) model of partial increment X-braced outrigger and braced-belt, a model of a virtual wall belt outrigger with partial increment (B32), and a model of a virtual braced-belt outrigger with partial increment (B33).

Results and discussion

Conventional outrigger

In this category, seven different structural models were studied, each having its own set of concrete and steel parameters, as well as variable outrigger and belt placements. Figures 21, 22, 23, and 24 show comparative graphs for lateral displacement, story drift, time period, and base shear for all response spectrum models studied. In a typical brace outrigger (B4), the highest lateral displacement after core (B2) is 63.2 mm, with a maximum story drift of 0.000641793 m and a minimum base shear of 6764 kN, as shown in figures. The least lateral displacement measured

(a)   **(b)**   **(c)**

Fig. 7 Conventional braced outrigger with **a** single-story brace belt depth, B11 **b** double-story brace belt depth, B12 **c** triple-story brace belt depth, B13

in a conventional wall outrigger with a wall belt (B5) was 29.9 mm, with a minimum story drift of 0.000345777 m and a maximum base shear of 6940 kN. With 3.58, 2.55, 3.14, 2.38, 2.47, 2.72, and 3 s time periods for B3, B4, B5, B8, B11, and B14, respectively, the value of lateral displacement is reduced by 39.8%, 16.4%, 44.6%, 42.2%, 31.9%, and 22% when compared to core (B2). When comparing B3, B4, B5, B8, B11, and B14 to the core (B2), story drift at the top of the building is reduced by 35.6%, 15.5%, 38.5%, 38.5%, and 18%, respectively. According to IS 1893 [32], the story drift should not exceed 0.004 times the story height. The base shear of each model varies slightly.

Conventional outrigger with belt depth

This category included thirteen alternative structural types, each with its own set of concrete and

steel requirements, as well as changing outrigger and belt placement and belt depth. For all models studied utilizing the response spectrum approach, comparative graphs for lateral displacement, story drift, time period, and base shear are shown in Figs. 25, 26, 27, and 28. The largest lateral displacement after core (B2) in a virtual brace outrigger with a single-story brace belt (B14) is 49.3 mm, according to the graphs, with a maximum story drift of 0.000519553 m and a minimum base shear of 6773.2 kN. With a minimum story drift of 0.000345777 m and a maximum base shear of 7158 kN, the least lateral displacement in a conventional wall outrigger with a triple-story wall belt (B7) was found to be 30 mm. When comparing B5, B6, B7, B8, B9, B10, B11, B12, B13, B14, B15, and B16 to core (B2), the reduction in lateral displacement was observed 43.8%, 48%, 53.4%, 44.3%, 41.4%, 46%, 34%, 25.7%, 46.8%, 23%, 24.5%, and 31.3% for 2.41, 2.59, 2.21, 2.50,
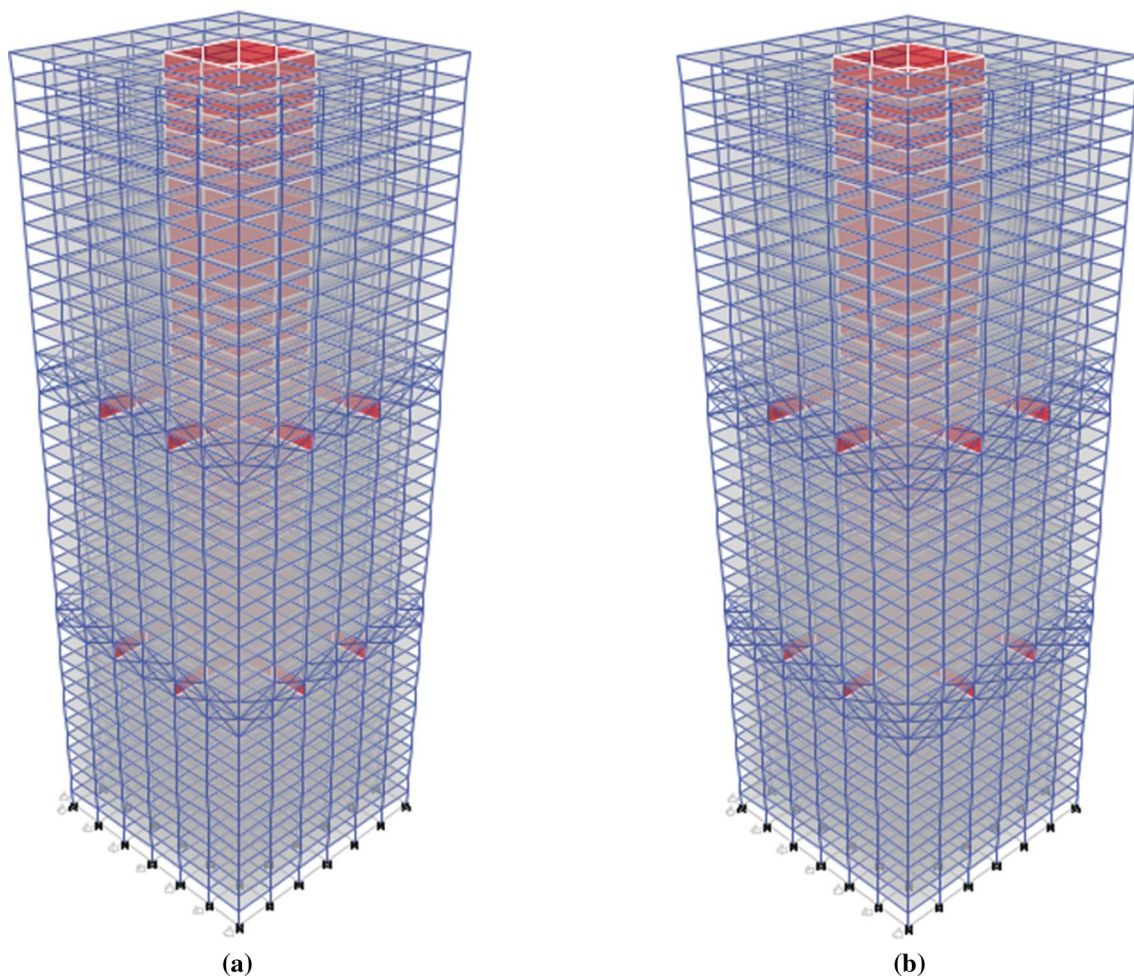
Fig. 8 Conventional wall outrigger with **a** double-story brace belt depth, B14 **b** triple-story brace belt depth, B15

2.39, 2.40, 2.69, 2.36, 2.32, 3.0, 2.91, and 2.83 s time period, respectively. Story drift at the top of the building is decreased by 40.5%, 41.4%, 44.0%, 36.0%, 37.7%, 41.4%, 25.8%, 35.7%, 40.5%, 18.6%, 21.8%, and 27.3% when compared to the core system (B2) with other buildings model such as B5, B6, B7, B8, B9, B10, B11, B12, B13, B14, B15, and B16. IS 1893 [32] states that the drift of a story must be less than 0.004 times the height of the story.

Virtual offset outrigger with belt depth

This category studied thirteen different types of structural models with diverse unique specifications of concrete and steel virtual outriggers with increasing depth and

virtual offset outriggers. For all models tested utilizing the response spectrum approach, comparative graphs for lateral displacement, story drift, time period, and base shear are shown in Figs. 29, 30, 31, and 32. In a B25 virtual offset outer brace outrigger, the maximum lateral displacement is 58.8 mm, the maximum story drift is 0.000606933 m, and the lowest base shear is 6762.7 kN, as shown in the graphs. Maximum base shear was 7085 kN, and the smallest lateral displacement was 33.4 mm for a virtual outrigger with a three-story wall belt (B19). The smallest story drift was 0.000381841 m. It is recommended that the drift between stories not exceed 0.004 times the height of the stories, as stated in IS 1893 [32]. When compared to core, the value of lateral displacement for B17, B18, B19, B20, B21, B22, B23, B24, B25, B26, B27, and B28 is reduced by 29.8%,
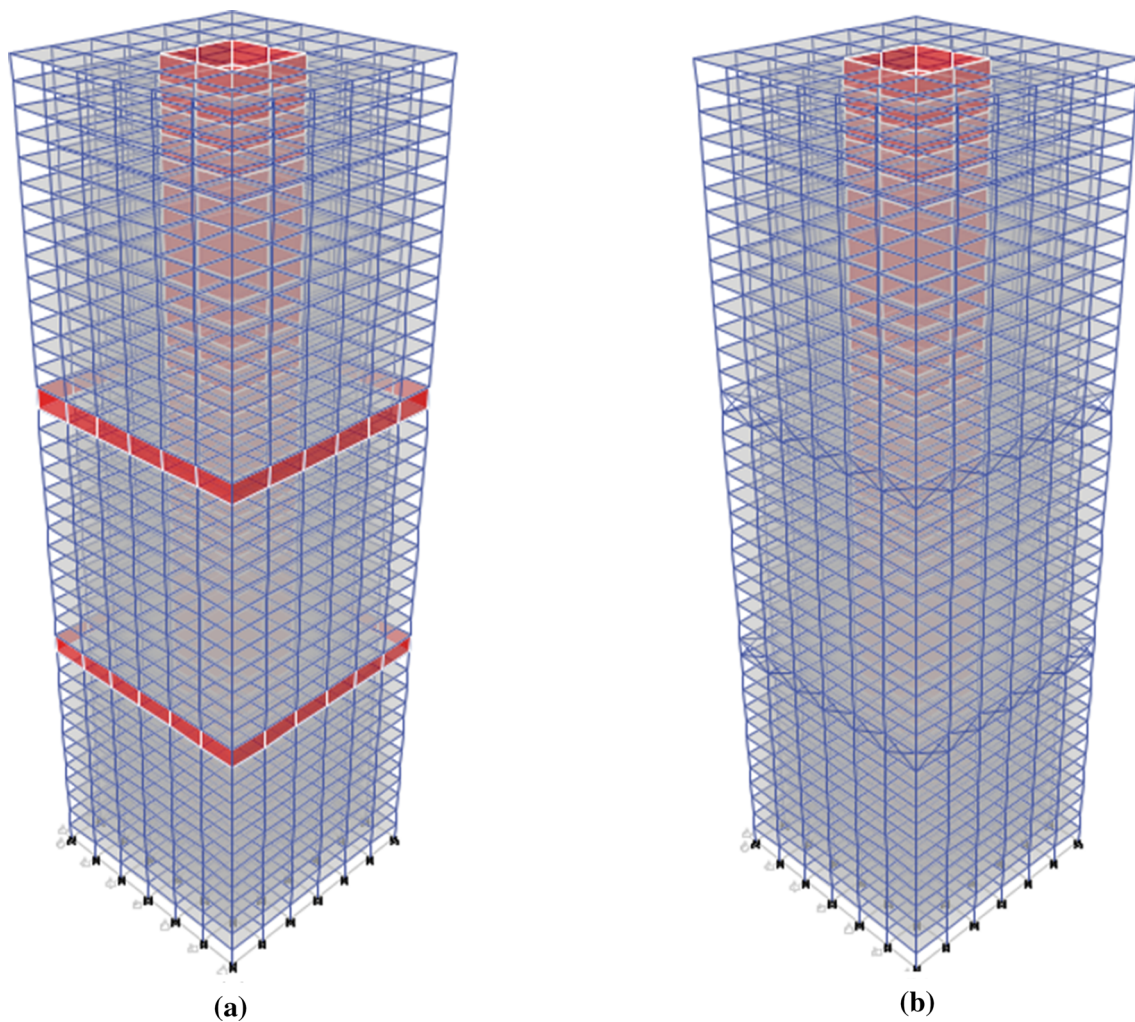
Fig. 9 Virtual outrigger with **a** single-story wall belt depth, B16 **b** single-story brace belt depth, B19

40.5%, 47%, 10.3%, 17.6%, 23.3%, 18.8%, 18.8%, 6.9%, 7%, 22%, and 11.2% with 2.78, 2.49, 2.31, 3.3, 3.11, 2.97, 3.57, 3.58, 3.57, 3.58, 3.57, and 3.58 s. Story drift at the top of the building is decreased by 26.3%, 37.2%, 38.8%, 7.5%, 16.5%, 21.3%, 15.4%, 16.2%, 6.2%, 6.2%, 17.4%, and 7.1% when compared to the core system with B17, B18, B19, B20, B21, B22, B23, B24, B25, B26, B27, and B28.

Conventional and virtual outrigger with partial depth

In this category, seven alternative structural models were examined, each with its own set of unique concrete and steel specifications, as well as partial outrigger and belt depth outrigger systems. For all models using the response spectrum approach, comparative graphs for lateral displacement, story drift, time period, and base shear are shown in Figs. 33, 34, 35, and 36. According to graphs, the greatest lateral displacement in a virtual brace outrigger with partial depth (B34) is 54.8 mm, with a maximum story drift of 0.000569745 m and a minimum base shear of 6773 kN. In a conventional wall outrigger with a belt and partial depth (B31), the least lateral displacement was found to be 34.6 mm, with a minimum story drift of 0.0003655 m but a maximum base shear of 7049 kN. When compared to core, the value of lateral displacement decreases by 44.2%, 19.6%, 51.3%, 26.3%,
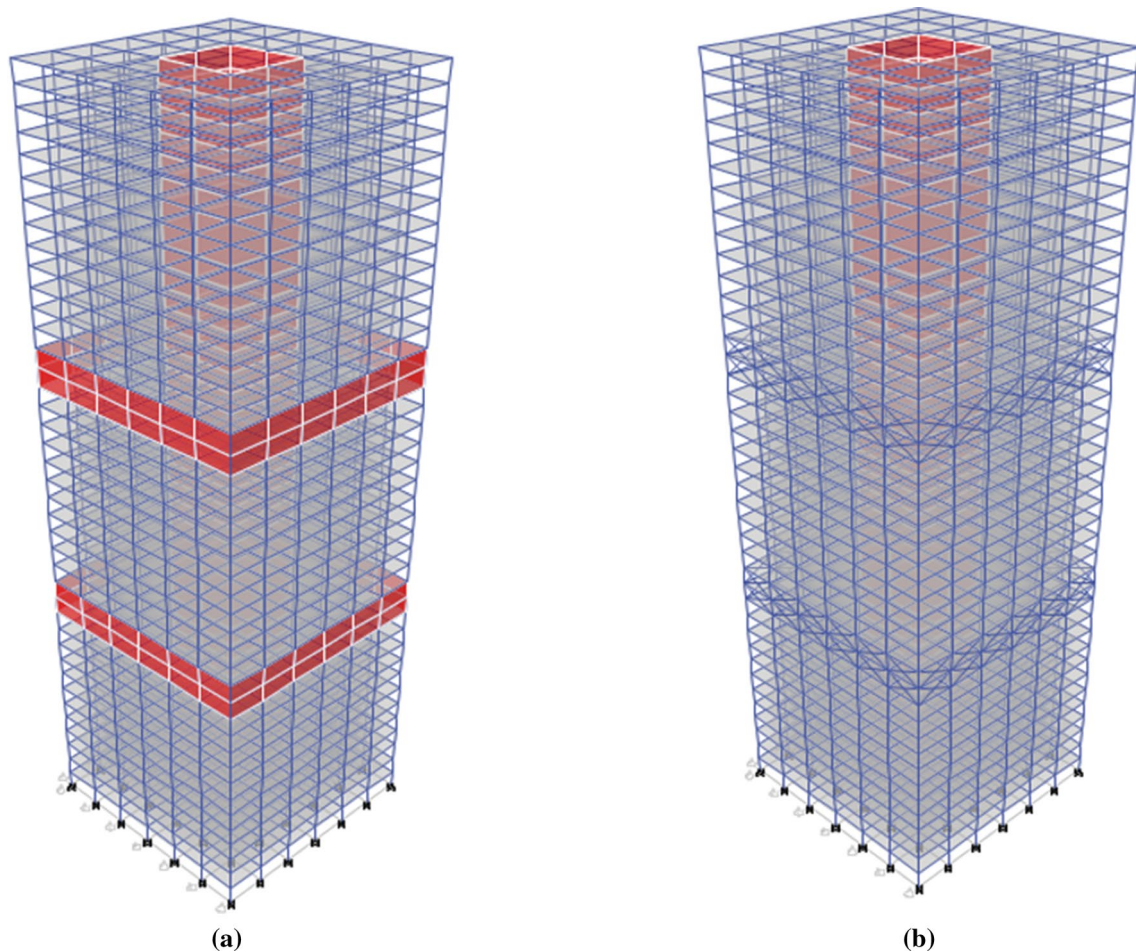
Fig. 10 Virtual outrigger with **a** double-story wall belt depth, B17 **b** double-story brace belt depth, B20

38.2%, and 13% with 2.43, 3.07, 2.26, 2.88, 2.56, and 3.24 s time periods for B29, B30, B31, B32, B33, and B34. Story drift at the top of the building is decreased by 37.9%, 18.4%, 41.3%, 23.6%, 33.4%, and 10.4% when compared to the core system with B29, B30, B31, B32, B33, and B34.

Load transferring mechanism of distributed belt

The belt engages and connects the adjacent and individual columns of the periphery to improve lateral load efficiency and direct more gravity load to the columns. The core system has no peripheral columns that contribute to lateral load (Fig. 37). In a traditional outrigger, an outrigger-restrained column adds lateral loads, while neighboring and corner columns do not (Fig. 38), but tying and engaging the periphery column solves the problem (Fig. 39). Under identical static analysis, a significant divergence in axial forces below and above the belt wall reveals the transfer of the core moment to the periphery column. When compared to the core system, using a wall outrigger and a brace outrigger increases axial forces by 66.4% and 47.5%, respectively, in an outrigger-restrained peripheral column. When utilizing a traditional outrigger and a belt wall, however, axial forces are reduced by 41% and increased by 70% at the outrigger-restrained column and corner column, respectively (Figs. 38, 39). When using a brace outrigger instead of a normal outrigger, axial forces are reduced by 24% and increased by 51.8% at outrigger-restrained columns and corner columns, respectively (Figs. 40, 41).
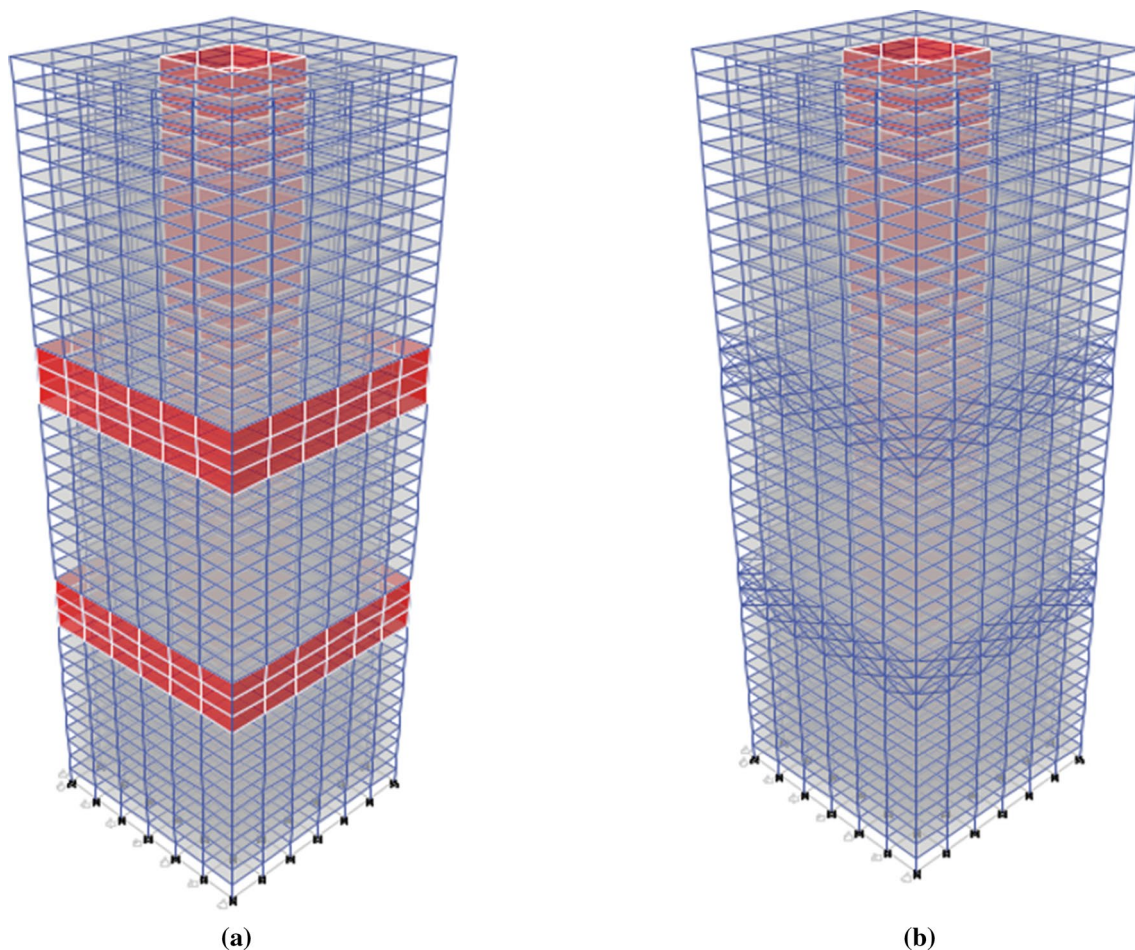
Fig. 11 Virtual outrigger with **a** triple-story wall belt depth, B18 **b** triple-story brace belt depth, B21

Variation under time history analysis

This category looked at six different structural models, all of which had positive results in the previous categories. Using El Centro vibration data, all models were analyzed using a time history approach, and comparison graphs for column axial load, acceleration, and velocity were generated (Figs. 42, 43, 44). Column force graphs show variation for the outrigger-restrained column on the 24th floor below the outrigger belt with the 15th number label, whereas velocity graphs show variation for the outrigger-restrained column on the 26th floor under the outrigger. The typical wall outrigger with triple-story depth (B7) absorbed more axial force than the other variations,

as shown in Fig. 42. Acceleration is reduced by 6.7%, 7.6%, 16.2%, and 10%, while velocity is reduced by 31%, 42%, 48%, and 46.7% for B7, B10, B19, and B31, respectively.

Conclusions

The purpose of this study was to perform linear and dynamic analyses, as well as nonlinear dynamic analyses, of conventional outriggers, conventional outriggers with belt depth, virtual offset outrigger belt depth, and conventional and virtual outriggers with partial depth under seismic load in order to gain a deeper comprehension
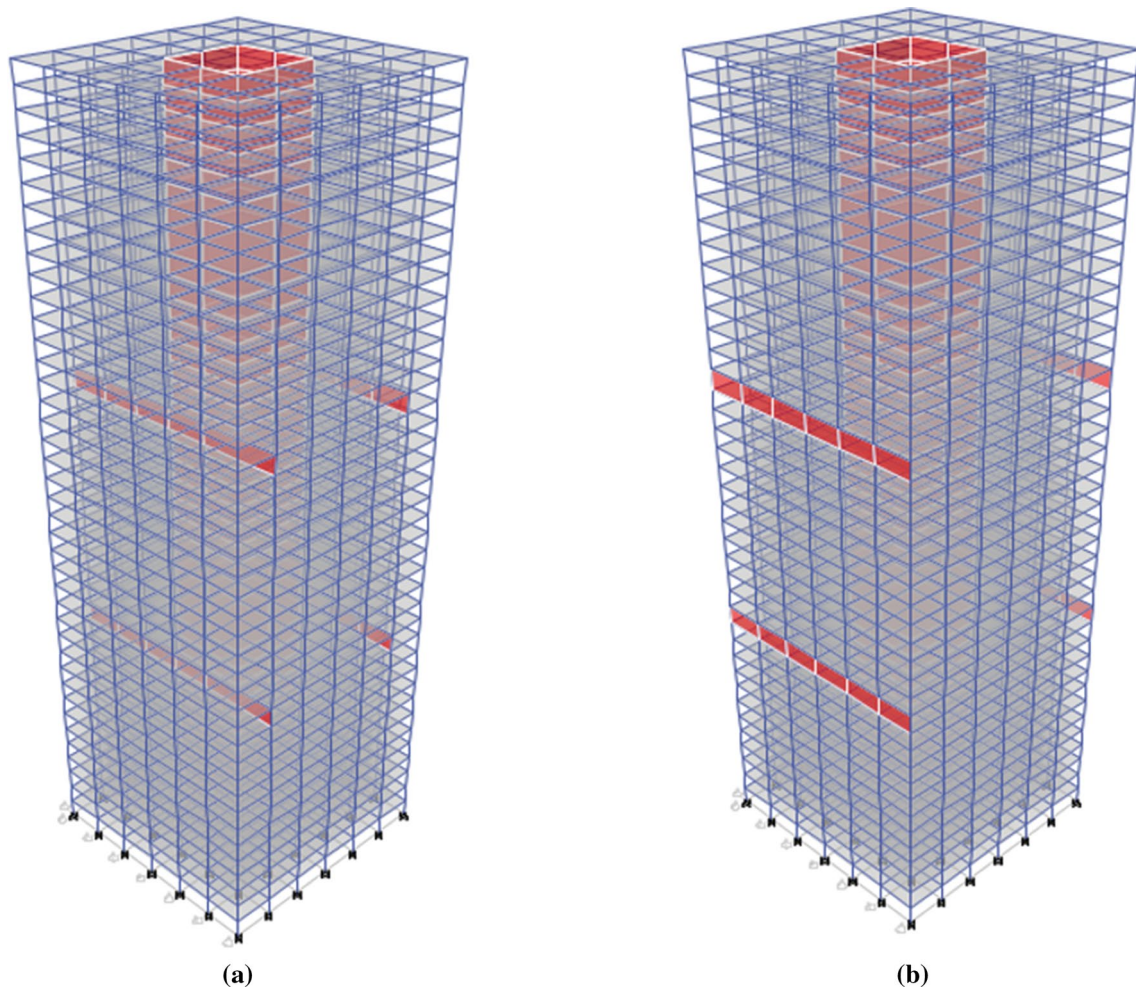
Fig. 12 Virtual offset wall **a** inner outrigger, B22, **b** outer outrigger, B23

of the functionality and load-transferring mechanism of distributed belt and conventional outrigger systems. This study also assessed the outrigger system in reinforced concrete structures to determine the safest path for load transmission and the most effective outrigger system in terms of depth on a 40-story reinforced concrete building. The following conclusions can be derived from the findings:

- In a brace outrigger system, the highest lateral displacement was 63.2 mm, with 0.6417 mm of story drift and 6764 kN of base shear. A conventional wall outrigger with a wall belt had 29.9 mm of lateral displace-

ment, 0.3457 mm of story drift, and 6940 kN of base shear. Compared to the core system, lateral displacement is decreased by 39.8% and story drift is reduced by 35.6%.

- The highest lateral displacement of 49.3 mm was observed in a virtual brace outrigger with a single-story brace belt, 0.5195 mm story drift, and 6773.2 kN base shear. The least lateral displacement in a typical wall outrigger with a triple-story wall belt was 30 mm, with a 0.3457 mm story drift and 7158 kN base shear. Lateral displacement decreased from 48 to 23%, and story drifts from 44.0% to 18.6%.

(a)

(b)
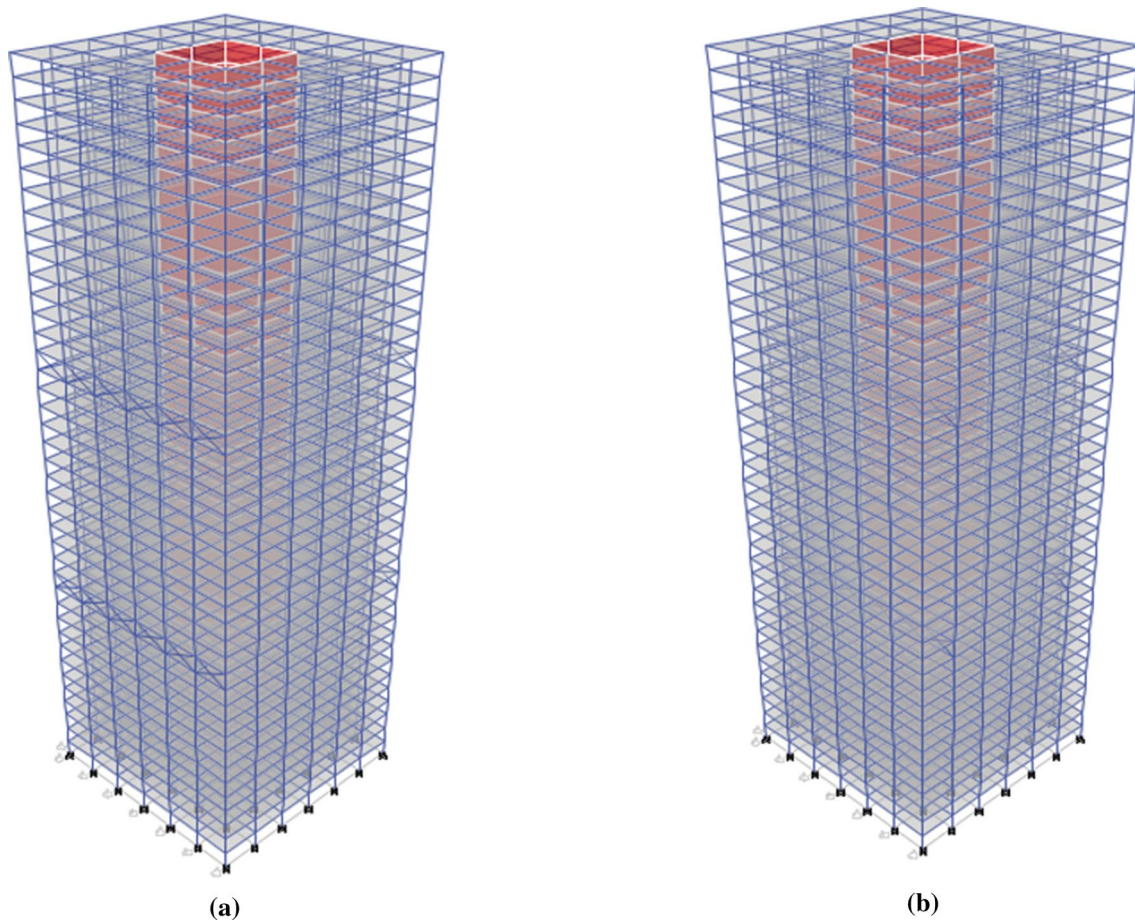
Fig. 13 Virtual offset brace **a** outer outrigger, B24, **b** inner outrigger, B25

- The virtual offset outer brace outrigger had 58.8 mm lateral displacement, 0.6069 mm story drift, and 6762.7 kN base shear. The minimum lateral displacement in a virtual outrigger with a triple-story wall belt was 33.4 mm, with a 0.3818 mm story drift and 7085 kN base shear. Comparatively, lateral displacement was reduced from 47% to 6.9%, and story drifts from 38.8% to 6.2%.
- A virtual brace outrigger with half depth, 0.5697 mm story drift, and 6773 kN base shear displaced 54.8 mm laterally. The least lateral displacement in a standard wall outrigger with a belt and partial depth was 34.6 mm, with 0.3655 mm of story drift and 7049 kN of base shear. Comparatively, lateral displacement reduced from 51.3% to 13%, and story drifts from 41.3% to 10.4%.

- A considerable divergence in axial forces below and above the belt wall exposes the core moment transmission. Using a wall outrigger and a brace outrigger increased axial forces by 66.4% and 47.5% compared to the core system. Traditional outriggers and belt walls reduced axial forces by 41% and increased them by 70% at the outrigger-restrained column and corner column, respectively. Using a brace outrigger instead of a conventional outrigger lowered axial forces by 24% and raised them by 51.8% at outrigger-restrained columns and corner columns.
- Time history curves depict the 26th-floor outrigger-restrained column's variations. Triple-story outriggers absorb greater axial force than other variations. Acceleration is reduced by 6.7%, 7.6%, 16.2%, and 10%, while velocity is reduced by 31%, 42%, 48%, and 46.7%.
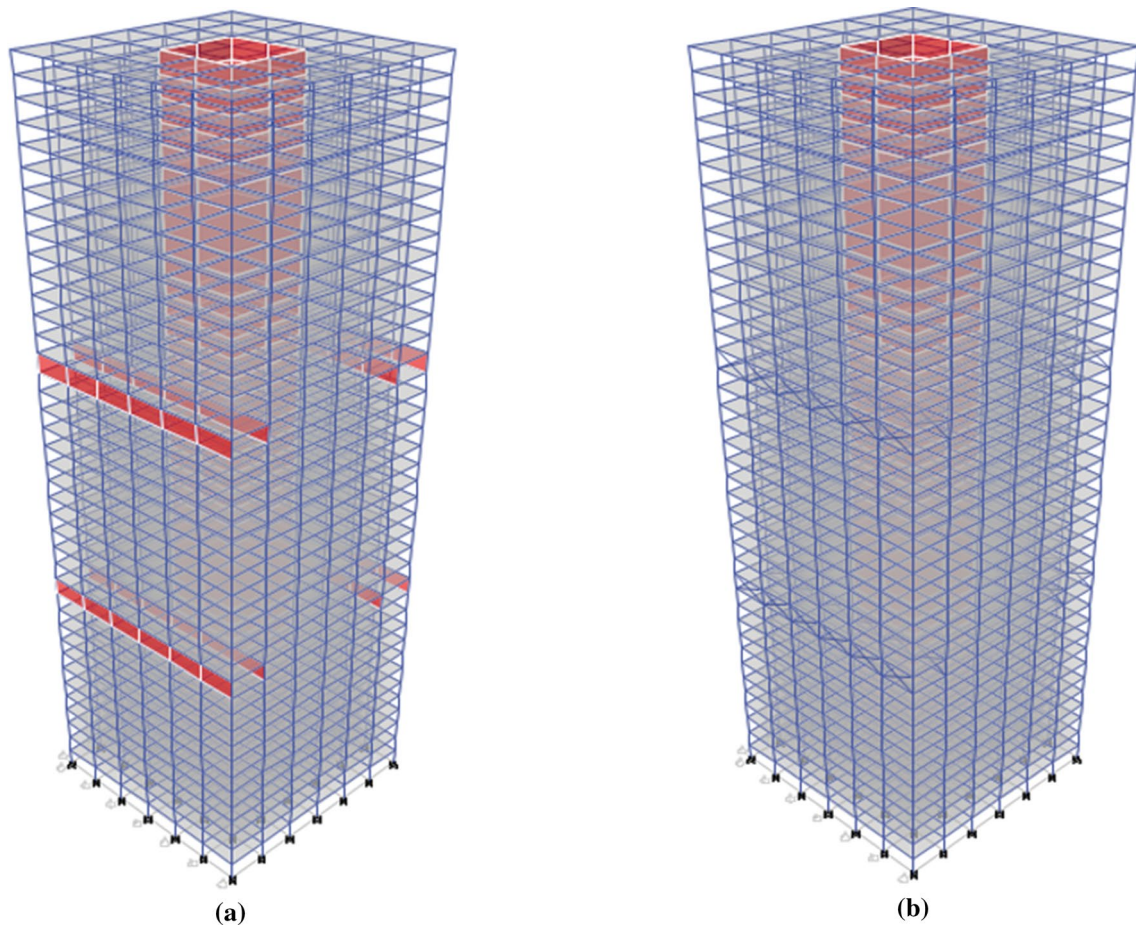
Fig. 14 Virtual offset **a** wall double outrigger, B26, **b** brace double outrigger, B27
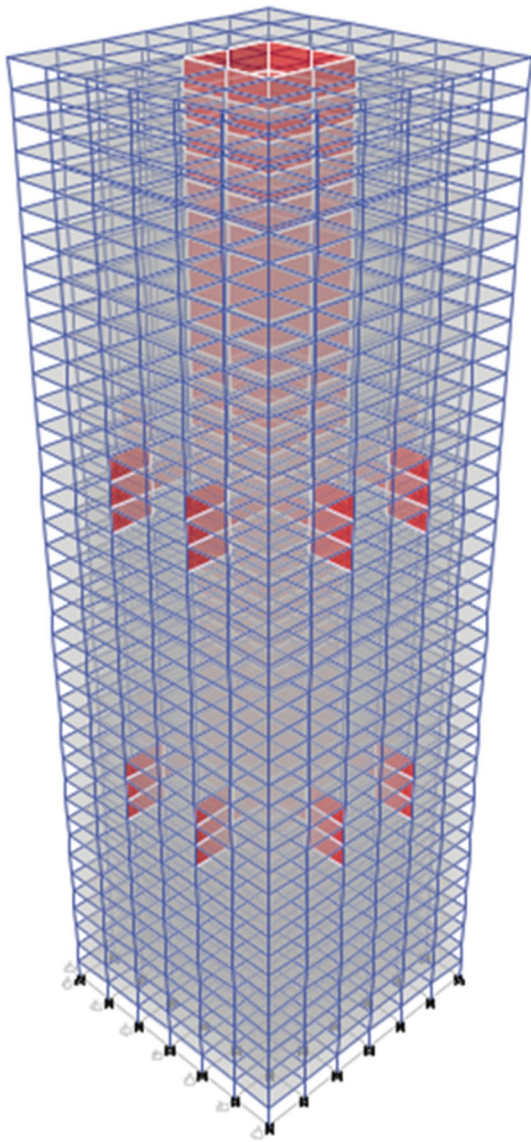
Fig. 15 Conventional wall outrigger with partial depth, B28
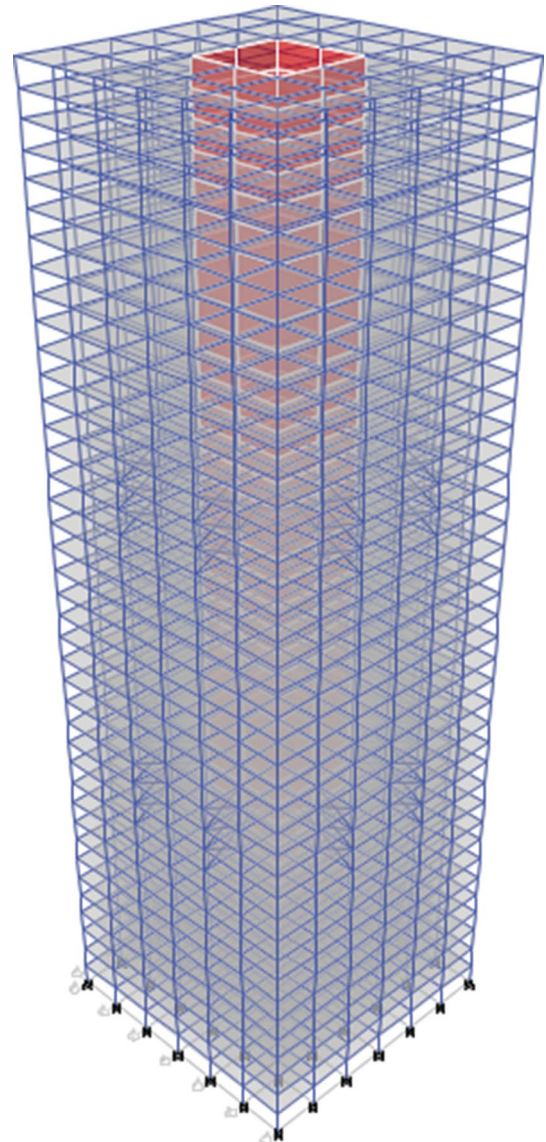
Fig. 16 Conventional brace outrigger with partial depth, B29
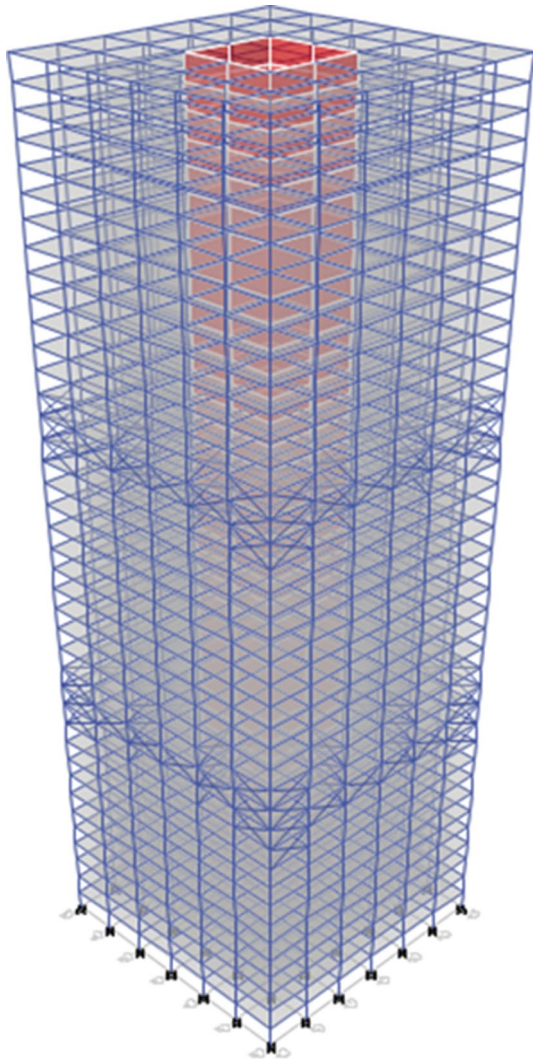
Fig. 17 Virtual brace outrigger with partial belt depth, B30
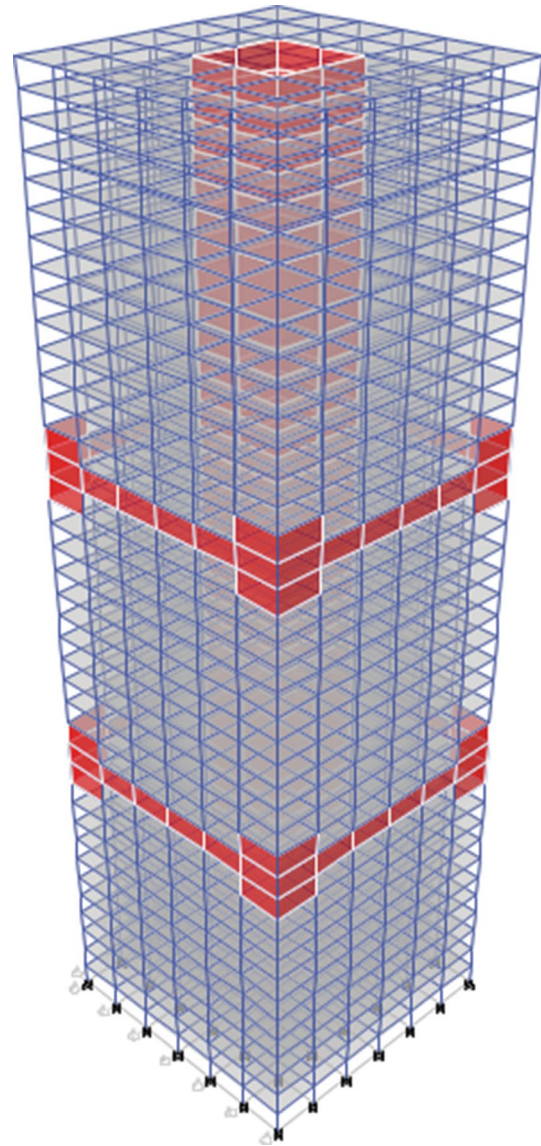
Fig. 18 Virtual wall outrigger with partial belt depth, B31
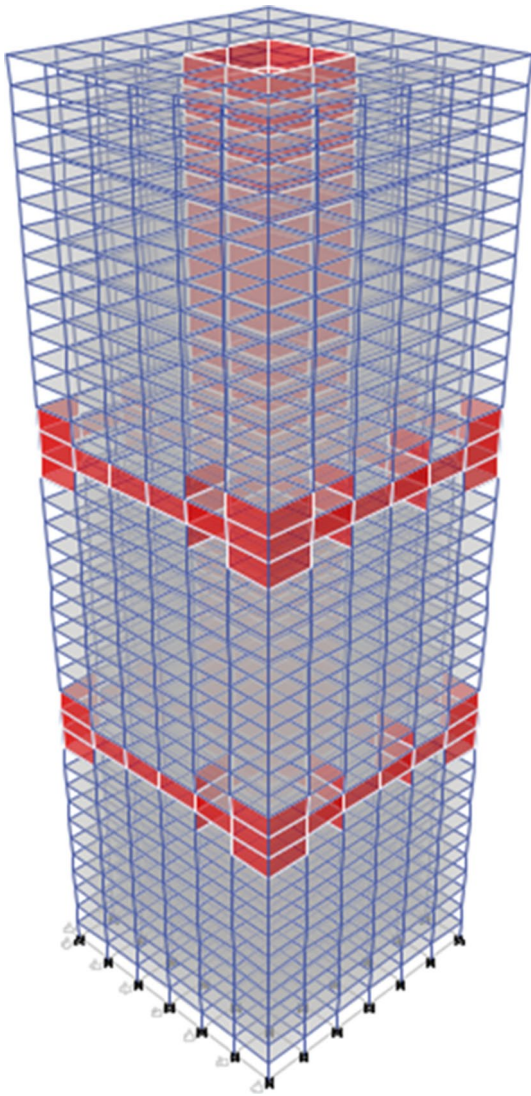
Fig. 19 Conventional wall outrigger with wall belt partial depth in both, B32
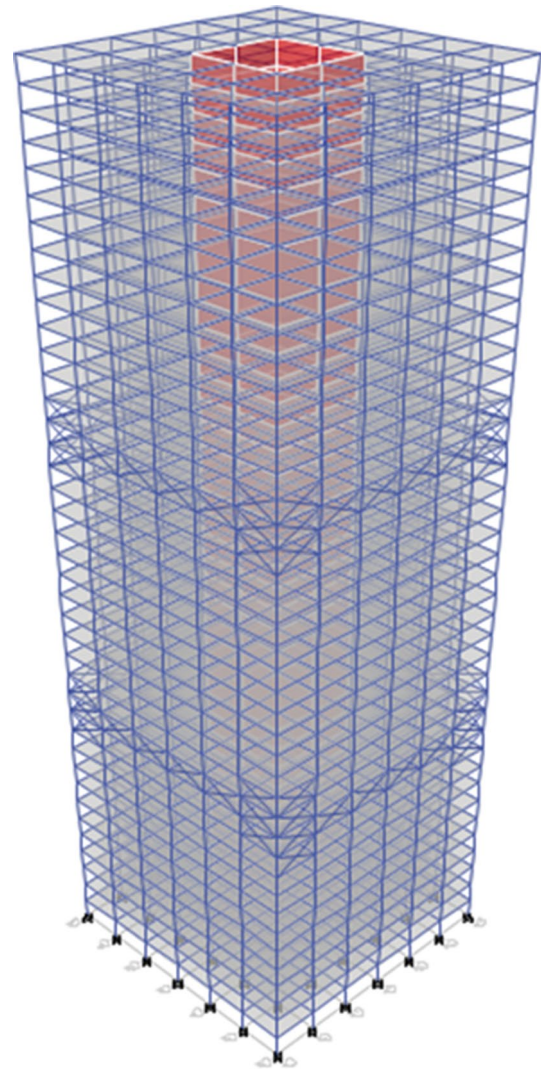
Fig. 20 Conventional brace outrigger with brace belt partial depth in both, B33
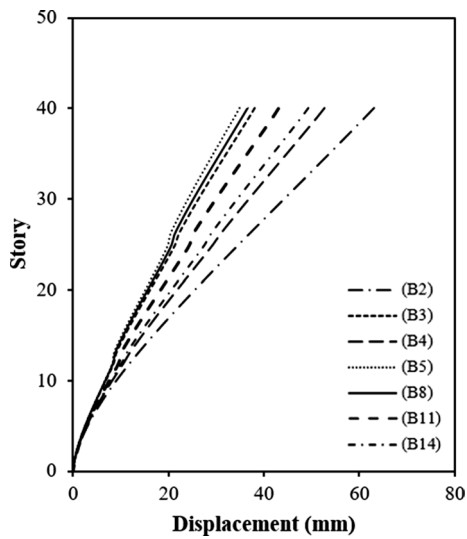
Fig. 21 Lateral displacement of conventional outrigger
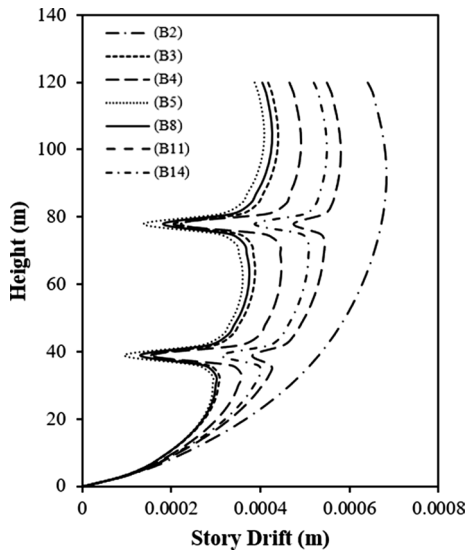
Fig. 22 Story drift of conventional outrigger
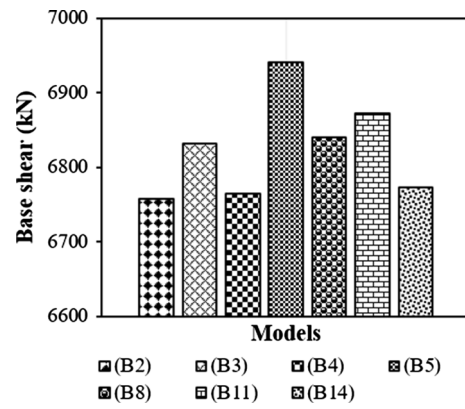
Fig. 23 Base shear of conventional outrigger
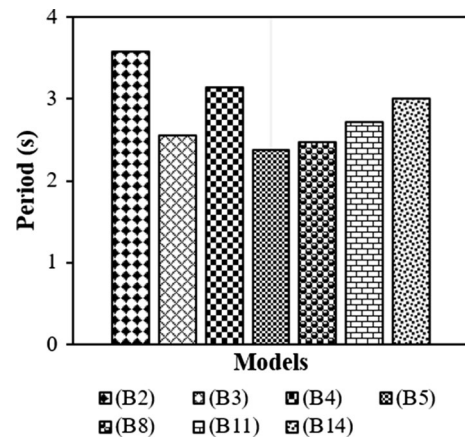
Fig. 24 Max time period of conventional outrigger
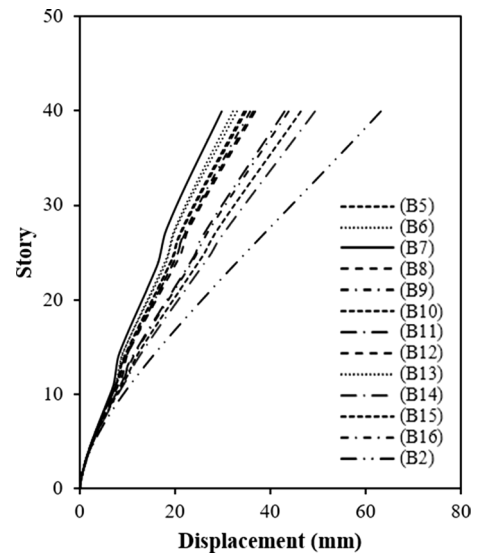
Fig. 25 Lateral displacement of conventional outrigger with belt depth
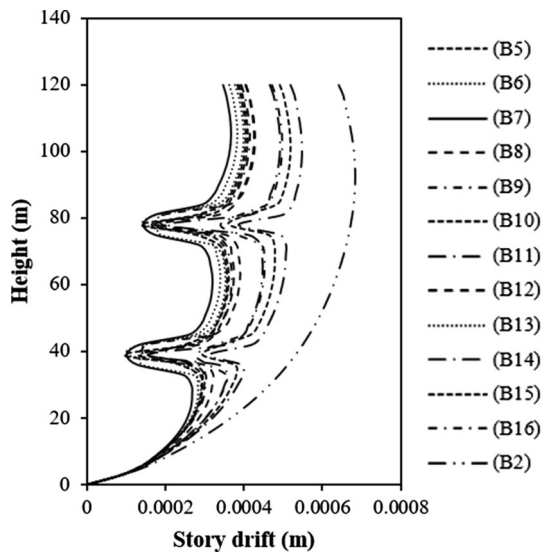
Fig. 26 Story drift of conventional outrigger with belt depth
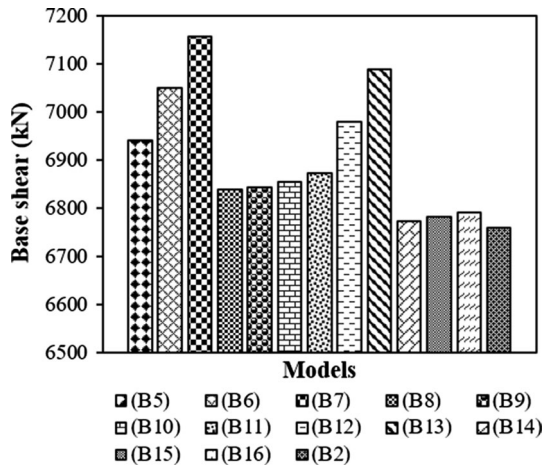
Fig. 27 Base shear of conventional outrigger with belt depth
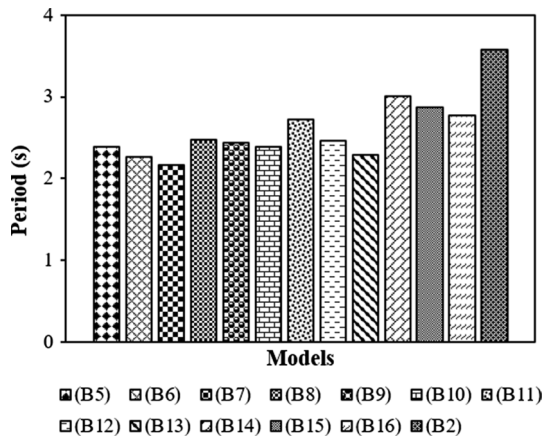
Fig. 28 Max time period of conventional outrigger with belt depth
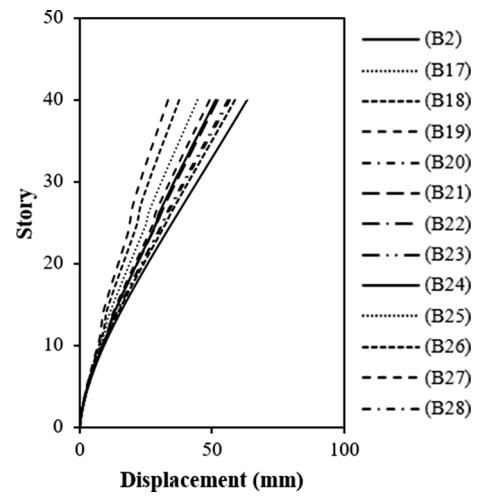
Fig. 29 Lateral displacement of virtual outrigger with belt depth
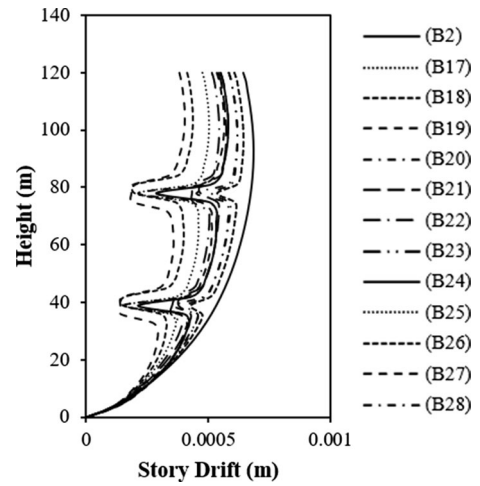
Fig. 30 Story drift of virtual outrigger with belt depth
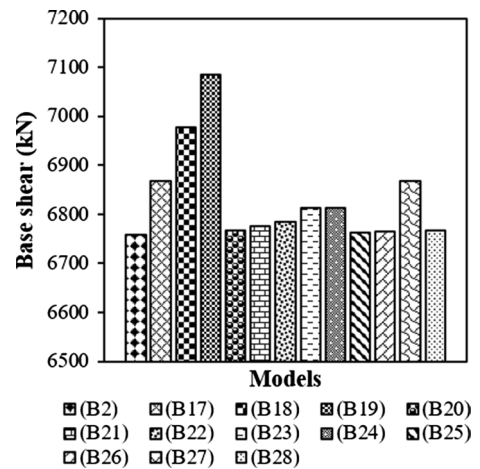
Fig. 31 Base shear of virtual outrigger with belt depth
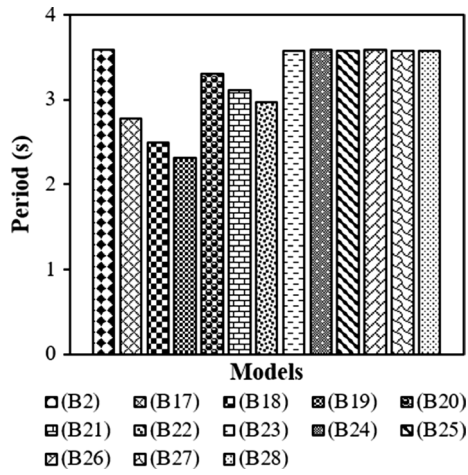
Fig. 32 Max time period of virtual outrigger with belt depth
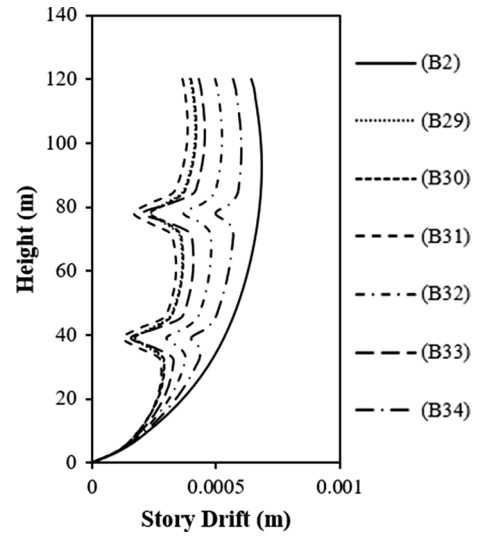
Fig. 34 Story drift of partial depth of conventional and virtual outrigger
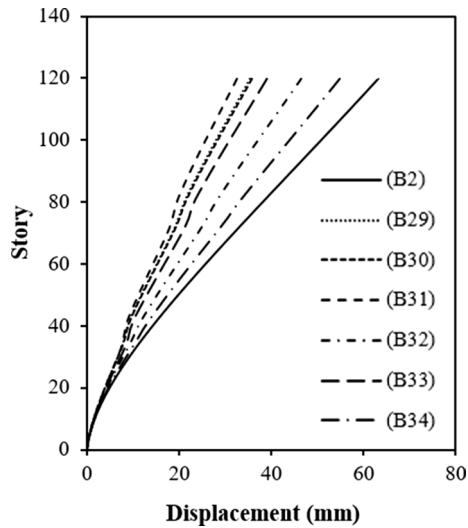
Fig. 33 Lateral displacement of partial depth of conventional and virtual outrigger
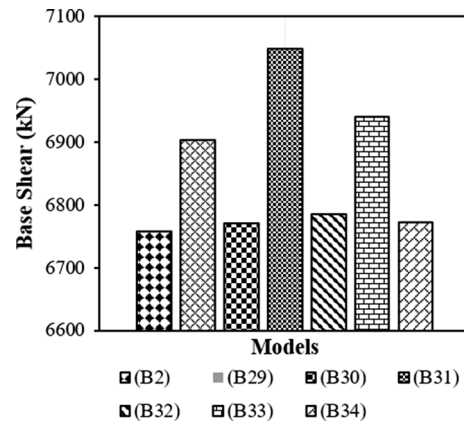
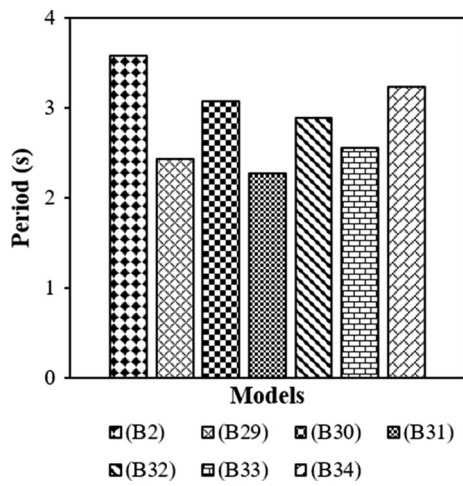**Fig. 35** Base shear of partial depth of conventional and virtual outrigger

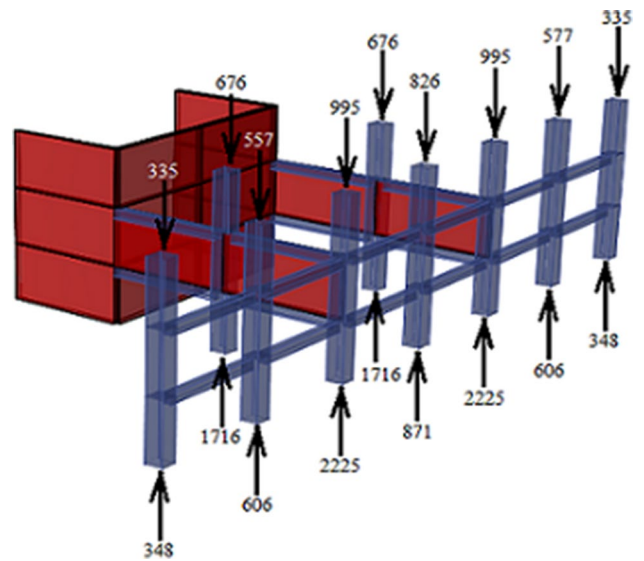**Fig. 36** Max time period of partial depth of conventional and virtual outrigger

Fig. 38 Internal forces in conventional wall outrigger
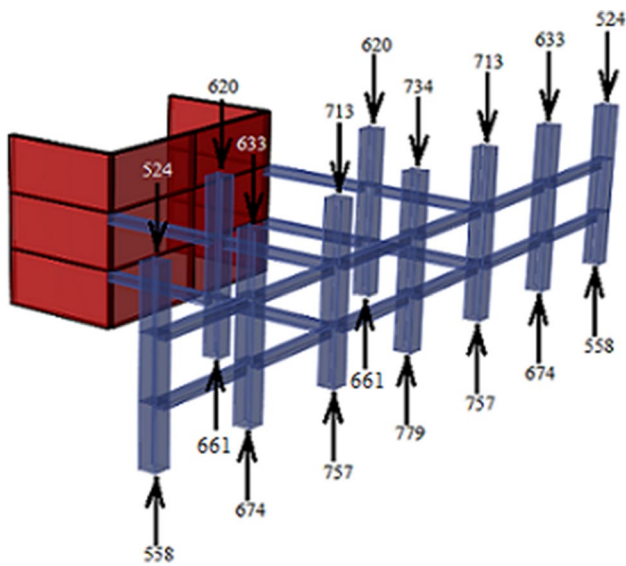

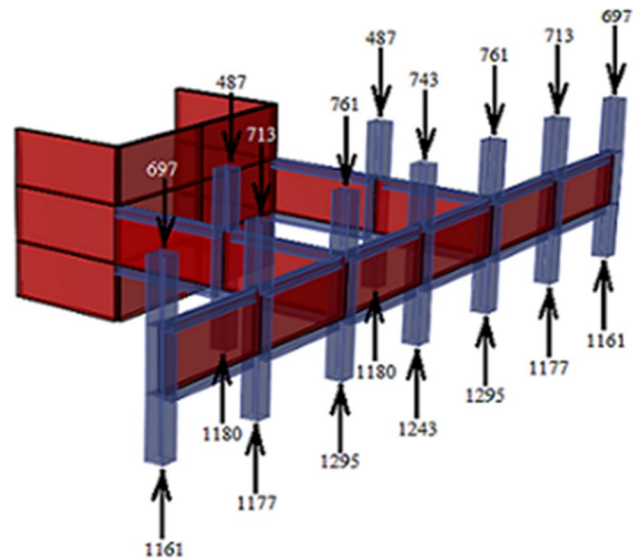**Fig. 37** Internal forces in core system

Fig. 39 Internal forces in conventional wall outrigger with belt wall
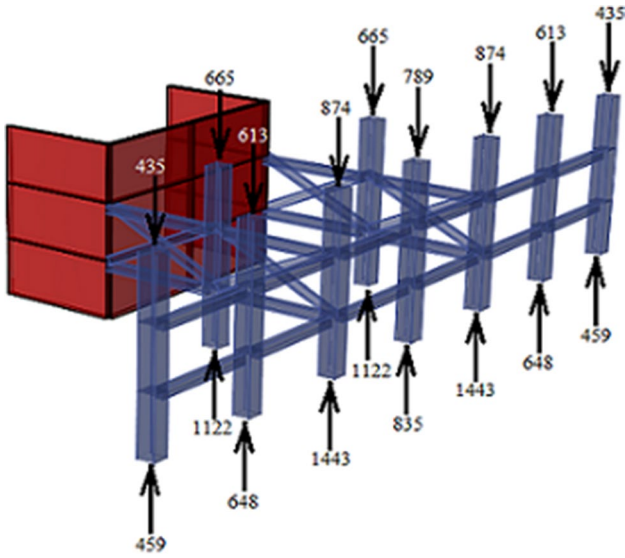
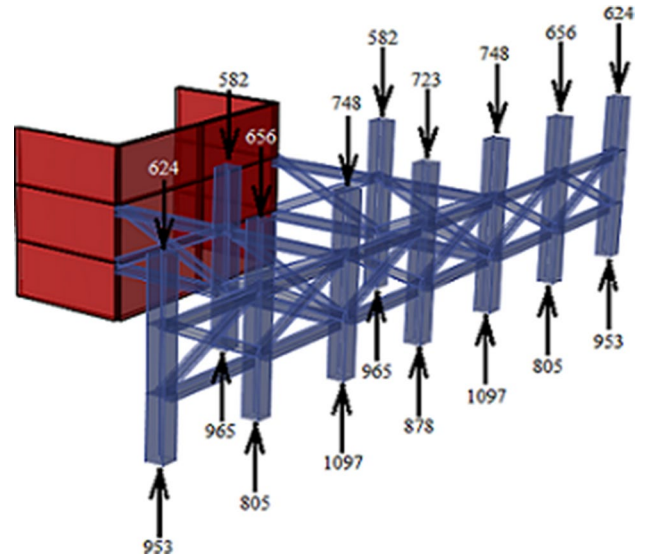**Fig. 40** Internal forces in conventional brace outrigger

Fig. 41 Internal forces in conventional brace outrigger with brace belt
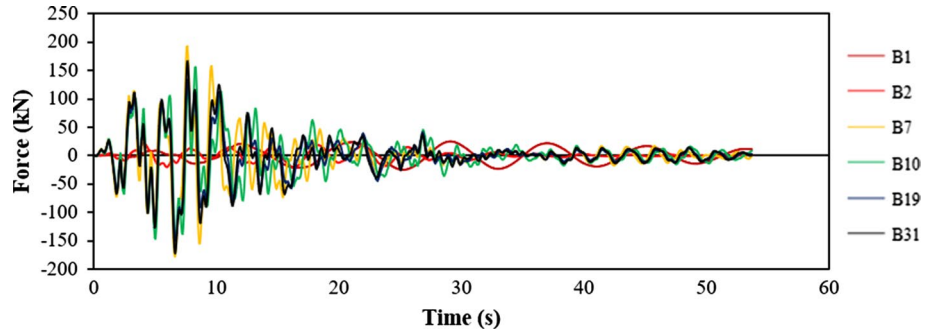
Fig. 42 Time history of column forces

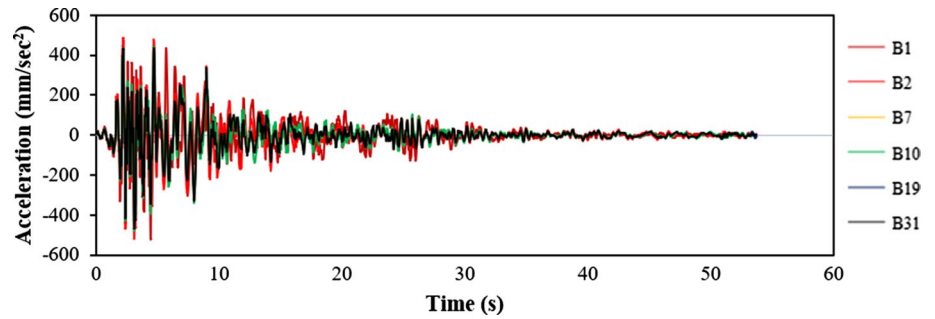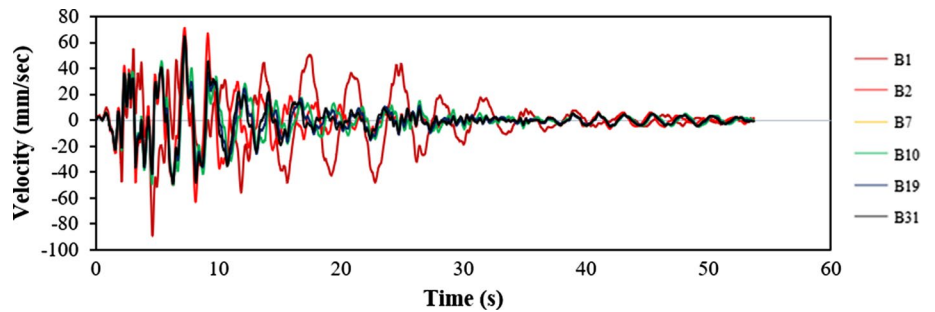**Fig. 43** Time history of acceleration

Fig. 44 Time history of velocity

Declarations

Conflict of interest On behalf of all authors, the corresponding author states that there is no conflict of interest.

References

1. Choi H, Ho G, Joseph L, Mathias N (2017) Outrigger design for high-rise buildings: an output of the CTBUH outrigger working group. Council on Tall Buildings and Urban Habitat, Chicago
2. Gan Vincent J.L., Chan CM, Tse KT, Lo Irene M.C., Jack Cheng, C.P. (2017) A comparative analysis of embodied carbon in high-rise buildings regarding different design parameters. J Clean Prod 161:663–675
3. Amoussou Cossi Prosper Dagbo, Lei Honggang, Alhaddad Wael, Halabi Yahia (2021) Simplified modeling and analysis method for skyscrapers with outrigger system. Structures 33:1033–1050. https://doi.org/10.1016/j.istruc.2021.04.096
4. Samadi M, Jahan N (2021) Comparative study on the effect of outrigger on seismic response of tall buildings with braced and Wall. Core II: determining seismic design parameters. Struct Design Tall Spec Build. 30:e1855. https://doi.org/10.1002/tal.1855
5. Salman K, Kim D, Maher A, Latif A (2020) Optimal control on structural response using outrigger braced frame system under lateral loads. J Struct Integr Maintenance 5(1):40–50. https://doi.org/10.1080/24705314.2019.1701799
6. Alavi A, Mele E, Rahgozar R, Farsangi EN, Takewaki I, Málaga-Chuquitaype C (2021) Uniform deformation design of outrigger braced skyscrapers: a simplified method for the preliminary design stage. Structures 31:395–405. https://doi.org/10.1016/j.istruc.2021.01.099
7. Fang B, Zhao X, Yuan J, Wu X (2018) Outrigger system analysis and design under time-dependent actions for super-tall steel buildings. Struct Design Tall Spec Build 27(12):e1492–e1520
8. Brunesi E, Nascimbene R, Casagrande L (2016) Seismic analysis of high-rise mega-braced frame-core buildings. Eng Struct 115:1–17
9. Beiraghi H, Siahpolo N (2017) Seismic assessment of RC core-wall building capable of three plastic hinges with outrigger. Struct Des Tall Spec Build 26(2):e1306–e1319
10. Kamgar R, Rahgozar R (2017) Determination of optimum location for flexible outrigger systems in tall buildings with constant cross-section consisting of framed tube, shear core, belt truss and outrigger system using energy method. Int J Steel Struct 17(1):1–8
11. Kamgar R, Rahgozar R (2015) Determination of optimum location for flexible outrigger systems in non-unifrom tall buildings using energy method. Iran Univ Sci Technol 5(4):433–444
12. Lin P-C, Takeuchi T, Matsui R (2019) Optimal design of multiple damped-outrigger system incorporating buckling-restrained braces. Eng Struct 194:441–457
13. Zhou Y, Zhang C, Lu X (2017) Seismic performance of a damping outrigger system for tall buildings. Struct Control Health Monit 24:e1864. https://doi.org/10.1002/stc.1864
14. Kafina R, Sagaseta J (2019) Analysis of outrigger-braced reinforced concrete supertall buildings: core-supported and tube-in-tube lateral systems. Struct Des Tall Spec Build 28:e1567. https://doi.org/10.1002/tal.1567
15. Kim HS, Lim YJ, Lee HL (2020) Optimum location of outrigger in tall buildings using finite element analysis and gradient-based optimization method. J Build Eng 31:101379. https://doi.org/10.1016/j.jobe.2020.101379
16. Lee J, Park D, Lee K, Ahn N (2013) Geometric nonlinear analysis of tall building structures with outriggers. Struct Design Tall Spec Build 22(5):454–470
17. Choi HS, Ho G, Joseph L, Mathias N (2012) Outrigger design for high-rise buildings, 1st edn. Routledge, New York
18. Patil DM, Sangle KK (2016) Seismic behavior of outrigger braced systems in high rise 2-D steel buildings. Structures 8:1–16
19. Kim HK (2015) Comparative analysis on influence of structure elements on optimal location of one-outrigger system. J Korea Inst Struct Maint Inspect 19(2):22–32
20. Kim HS (2018) Optimum locations of outriggers in a concrete tall building to reduce differential axial shortening. Int J Concr Struct Mater 12:77. https://doi.org/10.1186/s40069-018-0323-y
21. Fu F (2018) Design and analysis of tall and complex structures. Butterworth-Heinemann
22. Eom TS, Murmu H, Yi W (2019) Behavior and design of distributed belt walls as virtual outriggers for concrete high-rise buildings. Int J Concr Struct Mater 13:1. https://doi.org/10.1186/s40069-018-0311-2
23. Babaei M (2017) Multi-objective optimal number and location for steel outrigger-belt truss system. J Eng Sci Technol 12(10):2599–2612
24. Chen Y, Zhang Z (2017) Analysis of outrigger numbers and locations in outrigger braced structures using a multi-objective genetic algorithm. Struct Des Tall Spec Build 27(1):e1408–e1416
25. Chen Y, Cai K, Wang X (2018) Parameter study of framed-tube structures with outriggers using genetic algorithm. Struct Des Tall Spec Build 27(14):e1499–e1526
26. Kim HS (2017) Optimum design of outriggers in a tall building by alternating nonlinear programming. Eng Struct 150:91–97
27. Rahimi F, Aghayari R, Samali B (2020) Application of tuned mass dampers for structural vibration control: a state-of-the-art review. Civil Eng J 6(8):1622–1651
28. Rahem A, Djari Y, Noureddine L, Tayeb B (2021) Effect of masonry infill walls with openings on nonlinear response of steel frames. Civil Eng J 7(02):278–291
29. Computers and Structures, CSI-ETABS v17.0, Integrated Solutions for Buildings.
30. Taranath BS (2016) Structural analysis and design of tall buildings: Steel and composite construction. CRC Press, Boca Rotan
31. IS 13920 (2016) Indian Standard Code on Criteria for Earthquake Resistant Design of Structures. Bureau of Indian Standards: New Delhi, India
32. IS 1893 (2016) (Part-1); Indian standard code on criteria for earthquake resistant design of structures. Bureau of Indian Standards, New Delhi
33. IS 875 (1987) (Part-1); Indian standard code of practice for design loads (dead load) for buildings and structures. Bureau of Indian Standards: New Delhi, India.
34. IS 875 (1987) (Part-2); Indian standard code of practice for design loads (imposed load) for buildings and structures. Bureau of Indian Standards: New Delhi, India.